Multi-timescale Modeling and Dynamic Stability Analysis for Sustainable Microgrids: State-of-the-art and Perspectives

Mingyue Zhang, Yang Han, *Senior Member*, *IEEE*, Yuxiang Liu, Amr S. Zalhaf, Ensheng Zhao, Karar Mahmoud, Mohamed M. F. Darwish, and Frede Blaabjerg

***Abstract*—The increasing trend for integrating renewable energy sources into the grid to achieve a cleaner energy system is one of the main reasons for the development of sustainable microgrid (MG) technologies. As typical power-electronized power systems, MGs make extensive use of power electronics converters, which are highly controllable and flexible but lead to a profound impact on the dynamic performance of the whole system. Compared with traditional large-capacity power systems, MGs are less resistant to perturbations, and various dynamic variables are coupled with each other on multiple timescales, resulting in a more complex system in-stability mechanism. To meet the technical and economic challenges, such as active and reactive power-sharing, volt-age, and frequency deviations, and imbalances between power supply and demand, the concept of hierarchical control has been introduced into MGs, allowing systems to control and manage the high capacity of renewable energy sources and loads. However, as the capacity and scale of the MG system increase, along with a multi-timescale control loop design, the multi-timescale interactions in the system may become more significant, posing a serious threat to its safe and stable operation. To investigate the multi-timescale behaviors and instability mechanisms under dynamic inter-actions for AC MGs, existing coordinated control strategies are discussed, and the dynamic stability of the system is defined and classified in this paper. Then, the modeling and assessment methods for the stability analysis of multi-timescale systems are also summarized. Finally, an outlook and discussion of future research directions for AC MGs are also presented.**

***Index Terms*—Sustainable microgrid, hierarchical control, modeling, model simplification, multi-timescale, dynamic stability analysis, timescale decomposition.**

Received: October 26, 2023
Accepted: December 3, 2023
Published Online: May 1, 2024
Yang Han (corresponding author) is with the School of Mechanical and Electrical Engineering, University of Electronic Science and Technology of China, Chengdu 611731, China (hanyang@uestc.edu.cn).
DOI: 10.23919/PCMP.2023.000317

I. Introduction

With the increasing penetration of renewable and green distributed power generation in power systems, there are changes in the way the system generates, transmits, distributes, and uses electricity [1], [2]. A microgrid (MG) system, as a small-scale, low- and medium-voltage controllable distribution network, can operate in grid-connected and islanded mode, offering the possibility of efficient and flexible use of distributed energy, reducing the impact of intermittency of wind and solar energy on the main power grid, and making the power system more flexible, reliable, safe, clean and economical [1], [3]–[7].

A generic MG configuration consists of some common components such as distributed generators (DGs), energy storage equipment, loads, control equipment, communication facilities, etc., and is a single controllable entity relative to the power grid [3]. Unlike synchronous generators, most DGs have non-traditional forms of energy generation and need to be connected to the grid through interfaces such as power electronic converters [8]. These DGs usually need to power multiple classes of loads in the system, including linear passive, power electronic interface, and rotating motor interface loads [6]. With the increased participation of nonlinear loads, islanded MGs may face severe harmonic contamination at the point of common coupling (PCC) [9], [10]. Through a static transfer switch (STS) at the PCC the whole system is connected to the main grid and can be operated in grid-connected or islanded mode. When in islanded operation, frequency and voltage regulation are required to meet load demand and ensure system reliability. These can be implemented by each MG independently [3], [4], [7], [11], [12].

For the control architecture of the AC MG system, there are three main categories, i.e., centralized [13]–[16], decentralized [17], and hierarchical [5], [18]–28]. In centralized control, a dedicated central controller determines and optimizes the behavior of each

unit through the analysis of the data collected from each of them. Relying on extensive communication between the central controller and the controlled units, a precise balance between supply and demand can be achieved [7]. However, as a result of heavy dependence on communication links, the system has poor scalability and also faces challenges of delays, packet loss, and high cost of communication [21], [24], [29], [30]. Compared with centralized control, each unit in a decentralized control structure is controlled by its local controller and does not depend on the communication links. This reduces the cost of communication while providing the possibility of easy expansion. Thus, this control seems to be more suitable for MGs based on multiple DGs operating in parallel. However, as the number of DGs increases, the system is susceptible to power oscillation and inefficient energy utilization because of the lack of coordinated control between units. To address these issues for better energy management, multi-level control can be applied to MGs. In such a hierarchical control strategy, dedicated control algorithms can be applied to the corresponding control layers with necessary information/signal exchange between them, allowing large complex systems to be managed and controlled with targets using different timescales and technologies [5], [26]. However, the need for reliable communication links and the stability problems associated with the coupling of dynamics on different timescales also brings new challenges to this control with the increase of control layers. The details and characteristics of each control structure will be illustrated later.

Because of their advantages of flexibility, accuracy, and fast response in power conversion, power electronics converters have been widely used in MGs. However, unlike synchronous generators in traditional power systems, power electronic interface converters have no rotational inertia [31]. As a result, islanded MGs with small capacity and intermittent units are less robust and more susceptible to disturbance [3]. As a typical power-electronized power system, MGs have a longer timescale of dynamic variables than traditional AC power systems [32]. Because of the strong nonlinearities, the variables of the MG are coupled and interact at multiple timescales, and the physical phenomena at different timescales are no longer independent [33]. As the size and capacity of the system increase, the interaction of the various components in the system becomes more obvious, thus affecting the safe and stable operation of the MG system [6], [34]. Considering the above factors, the instability mechanism of MGs is more complex. Therefore, the applicability of existing power system modeling, analysis, and stability classification methods in the stability analysis of MGs needs further validation.

Accurate mathematical models are crucial for revealing the dynamic characteristics of MGs and the interactions between devices [18]. While accurately representing system characteristics, system modeling must take into account the complexity of the calculations. For different scenarios, the establishment of appropriate models is essential to reveal the instability mechanism and the critical influencing factors of the system and to realize accurate and efficient stability analysis. For the investigation of instability mechanisms in MG systems, there is a lack of standards for multi-timescale coupled reduced-order models (ROM) and quantitative analysis methods.

As for the stability analysis of MGs, there are two main analysis methods, i.e., small-signal and large-signal stability analysis. The small-signal stability analysis methods are generally based on equilibrium point linearization theory, which can be used to determine the asymptotic stability of the system at the equilibrium point and provide a basis for the design/optimization of system parameters. However, AC MGs are essentially time-varying, strongly nonlinear systems with complex coupled relationships between the equipment and the network, where the time variance is due to the switching action of the power electronics equipment and the time-periodic operating trajectory of the AC system and the nonlinearity is caused by the amplitude and duty cycle limitations in the closed-loop control system [35], [36]. Eigenvalue analysis methods based on the state space average model find it difficult to analyze the harmonics and their interactions during the electromagnetic transient process of the converters [37], [38]. To solve this problem, a generalized averaging method and harmonic state space approach are proposed to build a multi-frequency state-space model [36]–[41]. The generalized averaging model can be used to analyze the coupling characteristics between frequencies, but it cannot predict the frequency coupling issues between converters. The harmonic state-space model can capture such problems, but the modeling and analysis process is more complicated [36], [38]. Impedance analysis methods based on frequency domain criteria are widely used to analyze the interactive stability of MG systems with multiple converters [42]. However, impedance modeling is a typical black-box modeling approach with a difficult theoretical derivation of the model, especially for the grid impedance, which often lacks specific parameters [43]. Fortunately, the output impedance can also be measured by perturbed signal injection methods, and the model obtained has an equally good physical explanation [44].

The interactions within MGs become more complex when subjected to large disturbances, and, in addition,

small perturbations can be amplified into significant responses on a large scale during nonlinear evolution, causing system voltage and frequency collapse [33], [35], [45]. Although small-signal stability analysis based on linearization is easy to implement, the conclusions of the analysis are valid only near the equilibrium point of the system and cannot determine the boundaries of the stability domain or assess the stability margin of the equilibrium point. Therefore, it is critical to analyze and assess the transient stability of the system during large disturbances. At present, there are few studies on the large-signal instability mechanism and optimal controls of islanded MGs, especially transient stability analysis at the system level [35]. Although the dynamic interactions between power electronic devices have been studied through small-signal stability analysis, whether large-signal stability analysis can be used to analyze such interactions remains to be explored [46].

In the stability analysis of sustainable MG systems, the coexistence of different timescale components may generate a new instability mechanism [47]. Rational stability analysis is based on accurate classification of timescales [48]. As an example, voltage stability problems are usually related to slow dynamics and have been widely used for long and medium timescales [49]. However, the same issues may be induced by the line X/R ratio as well as the nonlinear load in multiple timescale systems [50]. Also, current controllers and other related factors significantly influence the voltage dynamics of the voltage source converters [48]. With the increasing size and capacity of MGs, it is necessary to explore the multi-timescale characteristics of MGs to gain insight into the dynamic characteristics of the system as well as the instability mechanism. The decomposition of the stability analysis in a timescale can be used to analyze the stability of multi-timescale systems such as MG systems [45], [47], [51]–[53]. Based on singular perturbation and stability domain theory, the method can be used to capture instabilities caused by interactions between fast and slow dynamics, avoiding wrong conclusions from transient and quasi-steady-state analyses [47], [51]. For example, based on singular perturbation theory, a slow-fast subsystem is established in [54], one which simplifies the sixth-order full model into a second-order slow subsystem and its small perturbation. Subsequently, the stability of both the slow and fast subsystems can be analyzed.

The rest of the paper is organized as follows. Section II describes the functions of each control layer of the hierarchical control for MGs in detail, and compares the advantages and disadvantages of various control strategies. Since the MG system has multi-timescale dynamics under a nonlinear structure, Section III reviews the modeling and simplification methods for small-signal and large-signal models, and the advantages, disadvantages, and applicability of each method are also discussed. Section IV classifies system stability based on the multi-timescale dynamical behavior of the AC MG system. Detailed descriptions, as well as simulation comparisons of the small-signal and large-signal stability analysis methods, are also presented. Section V discusses the future research trends of the AC MG system, including coordinated control, modeling, and stability analysis. The paper is concluded in Section VI.

II. Multi-timescale Hierarchical Control Framework of AC MG

Compared to traditional grids, MGs are more influenced by the natural resources and operating conditions and involve more dynamic variables at different timescales. This leads to new characteristics of stability, and poses great challenges for stable operation and efficient control. The objectives and core functions of an MG control system are [3]: 1) maintaining the voltages, currents, and frequency within acceptable limits; 2) keeping the power supply and demand balanced; 3) performing economic dispatch and demand-side management; and 4) switching between different operating modes.

Figure 1 shows the basic structure of an AC MG system, which can be categorized into three hierarchies with different functions and timescales, namely, primary, secondary, and tertiary [3]–[5], [7], [21], [29], [56], [57]. From the control signals issued by the upper control layer, the primary control realizes the power-sharing between DGs and ensures the stability of system voltage and frequency. This control layer is performed by the DG itself with a fast response, and is responsible for adjusting load fluctuations within seconds. The secondary control performs the function of controlling the load fluctuations in minutes and realizes power quality optimization, such as voltage and frequency recovery. In addition, the synchronization between the MG and the main grid, as well as transition control of islanded/ grid-connected modes, are also realized by this control layer. The tertiary control combines power generation and load predictions to realize the economic scheduling and energy storage management of the MG, providing references for the operation points and control parameters of each unit. This control layer is responsible for regulating load fluctuations at the hourly level. Secondary and tertiary controls are performed by the MG central controller (MGCC), as shown in Fig. 1. For stable operation of multi-loop control of the MG, the secondary and tertiary controls require low-bandwidth communication and are therefore slower to respond than the primary control.

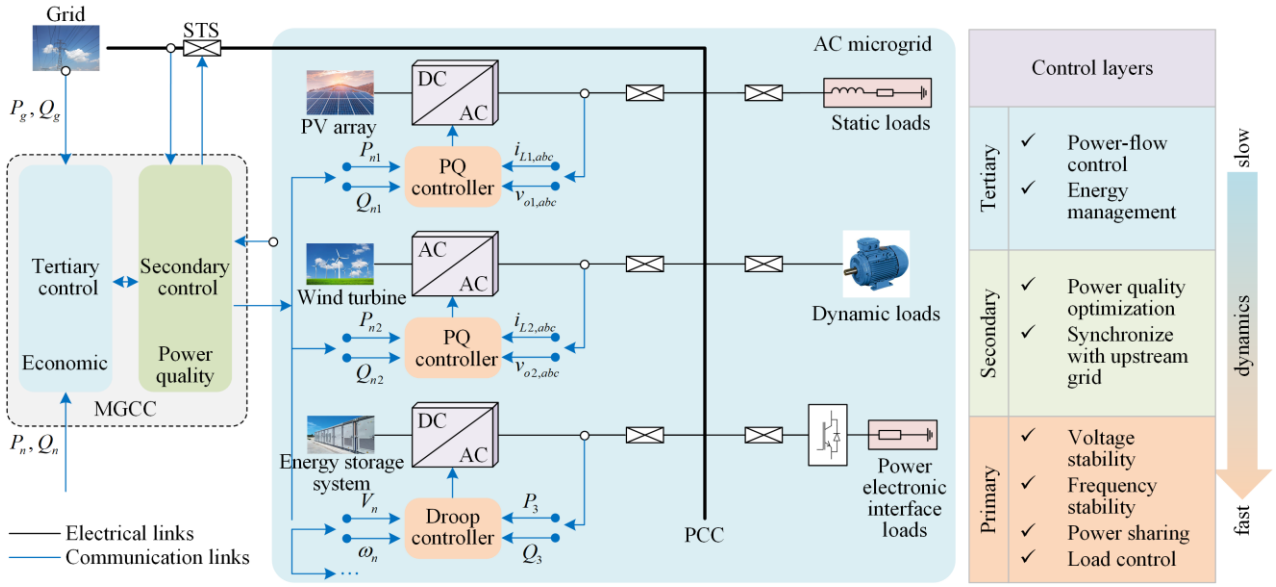

Fig. 1. Hierarchical and multi-timescale coordinated control configuration of the sustainable microgrid [1], [3], [5], [7], [25], [55].

With the increasing penetration of power electronic equipment in the system and the application of hierarchical control structures, MG systems face new network stability issues over wider bandwidths and more timescales. Taking the wind turbine generator (WTG) in an MG system as an example, the timescales of the AC MG system and the conventional power system with synchronous generators are compared, as shown in Fig. 2, including some representative time constants for typical facilities. It can be seen that the WTG exhibits a wider and more complex control bandwidth, highlighting its multi-timescale characteristics, particularly in the faster transient timescale. Based on this, the system in this paper is categorized into three timescales: transient, mid-term, and long-term. Also, in the light of the extensive adoption of voltage and current dual-loop control in existing AC MG research, a further division is made within the internal control, comprising terminal voltage control and current control. In the WTG system depicted in Fig. 2, the response of the current control is faster, followed by terminal voltage control, with both falling within the transient timescale range. In comparison, reactive power control exhibits a relatively slower response, belonging to the mid-term timescale range. To realize the decoupling between control layers, the bandwidth of the hierarchical control reduces in sequence from primary to tertiary control. This simplifies the design of the high-level controller and stability analysis and modeling of the system [5]. In addition, Fig. 2 also illustrates typical timescales of conventional power systems involving voltage and frequency regulation and stable operation. Notably, the MG system has a more complex and wider bandwidth, especially the control of current broadens the transient timescale, making the multi-timescale characteristics of the system more prominent [58].

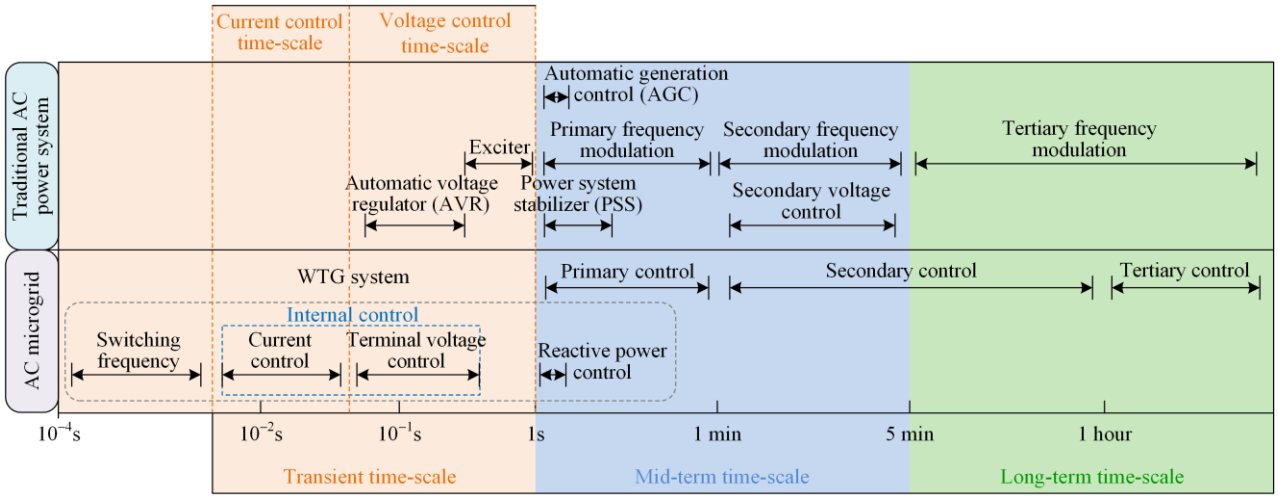

Fig. 2. Comparison of functions and their timescales of AC MGs and the traditional AC power systems [32], [35], [48], [57], [58].

A. Primary Control

In MG systems based on hierarchical control, the primary control is the innermost layer of the control hierarchy, and it is implemented by the converter interface controller of the DG. It has the fastest response in control layers. Each interface controller is achieved mainly by a cascade control system, including control loops of current, voltage, and external power [4], [5], [21]. To make each system variable track its reference signal accurately, the control of those variables is separated on different timescales [30]. Current and voltage control constitute the output control of the inverter, which has a fast response. As the outermost control loop, the power control loop aims to achieve the average power-sharing among DGs, and its response is slower than the first two. In the next part, power-sharing control methods based on centralized and decentralized characteristics will be compared and discussed.

1) Master-slave Control Based on Communication Links

In the master-slave structured MG, as shown in Fig. 3, one or more DGs of the MG act as the main power sources in the islanded mode under VF control to provide voltage and frequency support for the system while switching to PQ control in the grid-connected mode to output set power to the MG. In addition, the other DGs act as slave sources and always output set power to the MG based on PQ control in both grid-connected and islanded modes. When parallel/off-grid switching operation for MGs is necessary, the master power sources assume the primary responsibility: in the dual closed-loop control, the inner loop of current control remains the same, while the outer loop controller switches between VF and PQ control in order to achieve the control purpose in the operational mode. Then, the slave units act as auxiliaries and stay under PQ control during the transients. It should be noted that the PQ and VF controls of the master have the same current loops, but their reference signals are prone to change abruptly during switching, causing oscillations [56]. Also the same is true for the voltage phase angle reference signal. Therefore, smooth mode switching of master-slave control is essential to ensure power quality and system stability.

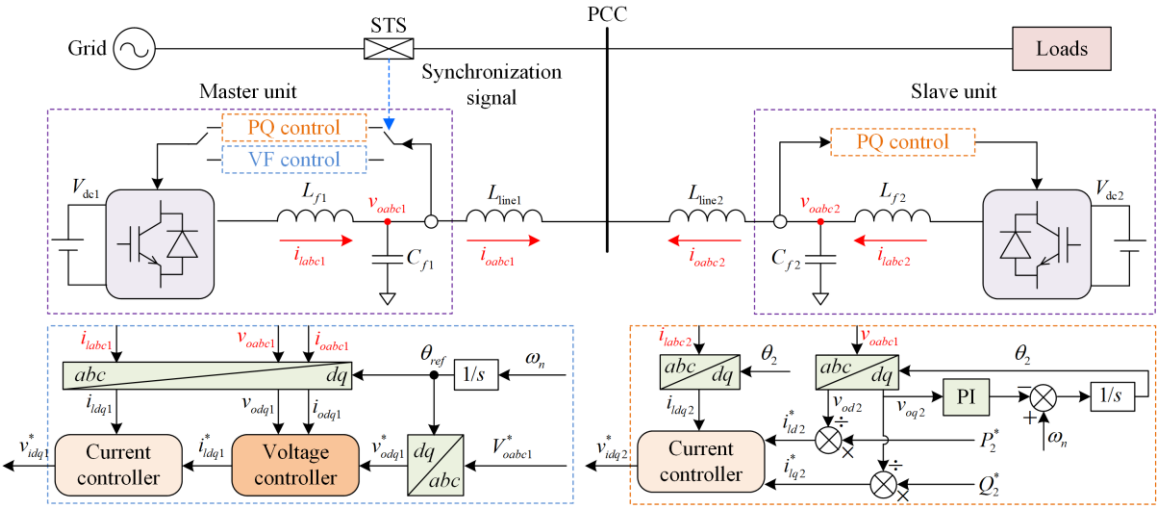

Fig. 3. The typical master-slave control structure of an AC MG [55], [59].

Based on low-bandwidth communication between units and a precise synchronization system, master-slave control has good power-sharing and frequency/voltage regulation performance. In addition, without the secondary control compensation, the voltage amplitude and frequency of the system can be maintained in the desired range. However, owing to the dependency on communication links, the system becomes less scalable and involves more construction cost [61], [62]. In addition, the overall global reliability of the system decreases, and the instability mechanism is complicated by increased interaction between units at different timescales [51].

2) Droop Based Control Techniques

To avoid the high cost and unreliability of the communication link, droop control participates in the system voltage and frequency regulation by introducing the droop characteristics of synchronous generators, with higher feasibility and expandability [45], [63]. A typical block diagram for droop control is shown in Fig. 4, and the principle of the power controller is given as:

$$\omega_i = \omega_{ni} - m_{pi}(P_i - P_{ni}),\ v_{oi}^* = V_{ni} - n_{qi}(Q_i - Q_{ni}) \quad (1)$$

where i is the index representing each inverter; and ω_{ni} and V_{ni} are the rated angular frequency and voltage amplitude, respectively; P_i and Q_i are the measured average active and reactive power values through the low-pass filter, respectively; while P_{ni} and Q_{ni} are the rated values of active and reactive power, respectively. These can be modified by the higher control layer; m_{pi} and n_{qi} are the active and reactive droop coefficients for a given voltage and frequency range, defined as:

$$m_{pi} = \frac{\omega_{i\max} - \omega_{i\min}}{P_{i\max}},\ n_{qi} = \frac{V_{oi\max} - V_{oi\min}}{Q_{i\max}} \quad (2)$$

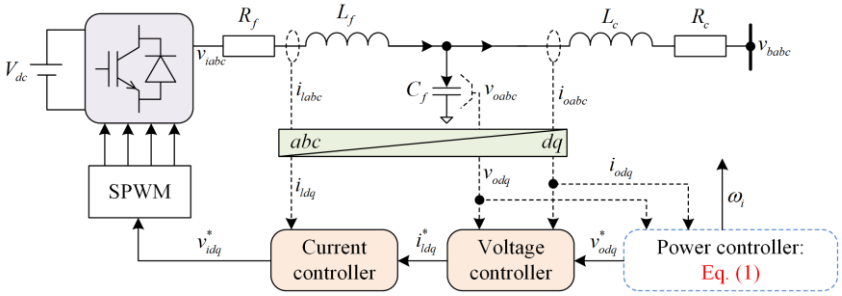

Fig. 4. Block diagram of inverter based on droop control strategy.

However, the design of the droop coefficients is not a simple quantitative process. A larger droop coefficient means better active and reactive power-sharing performance during load changes, with inherent deviations in frequency and voltage. These deviations cannot be eliminated by the droop control itself [22], [29]. This is especially the case in reactive power control, since the voltage is not a global variable in the system, and can lead to inaccurate reactive power-sharing [22]. In addition, the interactions among units will become significant because of the large droop coefficients, and the system is more prone to output current oscillation during sudden load change, which threatens stable operation. Therefore, the design of the droop coefficients should achieve a trade-off between power-sharing, voltage/frequency regulation performance, and system stability.

The derivation of (1) is based on the case of a purely inductive feeder, where the reference frequency is determined by the output active power, and the reference voltage by the reactive power [61]. This is true in traditional high-voltage transmission systems, whereas the line impedance in MGs and low-voltage distribution networks is predominantly resistive because of shorter line lengths and lower currents. The resistive impedance exhibits weaker coupling between active and reactive power because it has less dependence on frequency and primarily affects power transmission and losses. In the case of unknown line impedance, the coupling between active and reactive power control is further weakened because of the lack of accurate impedance values. The presence of unknown impedance may result in difficulties in accurately predicting current and power transmission behavior, thereby reducing the coupling effect between active and reactive power [4], [11], [22].

To enhance the adaptability of droop control, several improved forms have been proposed: 1) variation forms based on traditional droop control; 2) virtual-structure-based control; 3) auxiliary control; and 4) signal injection. These improved droop control schemes are discussed and compared in detail below. Signal injection technology can also be used as the power-sharing mechanism for MG systems. However, because of the complexity of implementation and output power variation caused by signal injection, the practical value of this method still needs to be verified [30].

a) Variation Forms Based on Traditional Droop Control

VPD/fQB control [25], [62] and angle droop control [45], [62], [64] are typical variations of the traditional droop control. The method replaces the original active and reactive droop characteristics with VP droop and FQ boost characteristics, and is applicable to low-voltage MGs with resistive line impedance. The control functions can be expressed as:

$$v^*_{oi} = V_{ni} - n_{pi}(P_i - P_{ni}),\ \omega_i = \omega_{ni} - m_{qi}(Q_i - Q_{ni}) \quad (3)$$

where n_{pi} and m_{qi} are the active and reactive droop coefficients in *VPD/fQB* control, respectively. However, the application of *VPD/fQB* control is limited by the line parameters of the MG system, and the accuracy of active power-sharing cannot be guaranteed [62]. In the traditional P/ω droop mechanism, the dynamic performance of the control is restricted by the frequency range of the system, which means that the control response is slow and may not be able to quickly adapt to transient events within the MG. Therefore, the latter replaces it with the P/δ droop characteristic to adjust the active power-sharing [45], [62]. This power-sharing mechanism, also known as angle droop control, adjusts the active power allocation based on the variation of phase angle δ. By using the changes in phase angle, P/δ control can better reflect voltage phase variations and enable more efficient power sharing. Hence, P/δ control demonstrates superior performance and adaptability, enhancing power sharing in MGs. Mathematically, the P/δ droop control can be expressed as:

$$\delta_i = \delta_{ni} - m_{pi}(P_i - P_{ni}) \quad (4)$$

where δ_{ni} is the rated voltage phase angle of converter i. This control has a good performance for active power-sharing, and the system frequency would not drop significantly when the load increases. However, because of the lack of frequency synchronization between the converters, the phase angle difference may diverge, leading to system instability [22], [62].

b) Droop Control Based on Virtual Structures

Virtual structure-based droop control mainly includes generalized droop [65], virtual impedance [9], [10], [66]–[68], and virtual synchronous generator (VSG) control [69], [70]. With complex line impedance, the generalized droop control uses orthogonal linear rota-

tional transformation matrices to modify active and reactive power P and Q to approximate the case of purely inductive lines, e.g., [65]:

$$\begin{bmatrix} P_{di} \\ Q_{di} \end{bmatrix} = \begin{bmatrix} \sin\theta_i & -\cos\theta_i \\ \cos\theta_i & \sin\theta_i \end{bmatrix} \begin{bmatrix} P_i \\ Q_i \end{bmatrix} \tag{5}$$

where θ_i is the line impedance angle. Thus, X and R of the power line are required to determine θ. On the other hand, virtual impedance control can also be used to decouple active and reactive power control without physical elements. In virtual impedance control, the output impedance of the DG is regarded as a controllable variable, and the voltage reference signal of the inverter can be expressed as [60]:

$$v_{\text{ref}} = v_{oi}^{*} - Z_{\text{D}}(s) i_{\text{o}} \tag{6}$$

where $Z_{\text{D}}(s)$ is the transfer function of the virtual impedance; and i_{o} is the output current. Using this method, the influence of resistive [22] and mismatched feeder impedance [68] on power-sharing is reduced. In addition, harmonic compensation can be achieved by introducing virtual impedance on the harmonic frequency [9], [10]. However, the introduction of virtual impedance control reduces the output power quality of the inverter, and the weak damping property of the algorithm can also affect the stability margin of the MG system. In particular, in the weak grid condition, the virtual impedance control strategy may lose efficacy because of the dynamic influence of the phase-locked loop (PLL) [71].

The concept of VSG control, which adds virtual inertia to the power system by controlling VSCs to emulate the behavior of the synchronous generators, is recognized as an effective measure to solve the potential stability issues of such systems [67], [72]–[74]. The mathematical equations of active and reactive power controls in VSG control are given as [73]:

$$J\frac{\mathrm{d}\omega_i}{\mathrm{d}t} = \frac{P_m - P_e}{\omega_i} + D(\omega_n - \omega_i),\ K\frac{\mathrm{d}E_r}{\mathrm{d}t} = Q_m - Q_e + n(V_n - v_i) \tag{7}$$

where J, D, K, and n are the equivalent moment of inertia, damping, inertia and droop coefficients, respectively; E_r is the virtual electromotive force; P_m, P_e, Q_m, and Q_e are the mechanical and electromagnetic active and reactive power of VSG, respectively. By strengthening the converter's support to the voltage and frequency of the grid, the VSG control enhances the accessibility of the grid interconnection of DGs. However, the converter based on the VSG scheme is a power electronic piece of equipment, and its anti-disturbance performance is not the same as that of traditional synchronous generators, and is prone to frequency or power fluctuation when subjected to disturbances [69].

TABLE I
ADVANTAGES AND DISADVANTAGES OF TYPICAL PRIMARY CONTROL METHODS FOR MICROGRID

Control methods			Advantages	Disadvantages
Master-slave control	VF-control [56], [61], [76]		√ The structure is simple and easy to implement √ Good power-sharing and voltage regulation in steady-state	× High-bandwidth communication requirements × High current transient during mode transition × Poor reliability, redundancy, and scalability
	PQ-control [8], [56], [61], [76]			
	Traditional form [6], [8], [57], [61], [77]–[84]		√ Easy implementation without communication √ Modularity, high reliability, flexibility, and scalability	× Sensitive to line parameters × Deviation of V and f × Poor harmonic sharing performance × Transient response is slow
	Variations	*VPD*/*fQB* droop control [25], [60]	√ For highly resistive power lines	× Affected by system parameters × Inaccurate active power-sharing
		Angle droop control [45], [62], [64]	√ For constant frequency regulation √ Good transient performance of active power-sharing	× DGs require synchronization with each other
Droop control	Virtual structure-based control	Generalized droop control [65]	√ Not affected by line parameters	× Line parameters are required
		Virtual impedance control [9], [10], [50], [66]–[68]	√ Not affected by line parameters √ Good harmonic sharing performance	× Poor output power quality × Affected the stability margin of the system
		VSG control [69], [70]	√ Optimized inertia and damping of the system	× The anti-disturbance performance is not as good as traditional synchronous generators
	Auxiliary control	Adaptive droop control [30]	√ Better power-sharing and circulating current minimization	× Line parameters are required
		Transient droop control [12]	√ Improved the stability margin of the system	× Changed the original pole-zero location of the system
		Auxiliary loop [62], [85], [86]	√ Improved system damping	× Transient reactive oscillations

c) Droop Control with Auxiliary Control

This method mainly includes adaptive droop [30] and transient droop control [12], and other droop control with an auxiliary loop [64], [75]. The adaptive droop control is mainly proposed and applied to achieve better power-sharing and circulating current minimization. An adaptive droop control method is proposed in [30]. This introduces an adaptive differential term into the traditional droop characteristics and optimizes the dynamic performance of power-sharing with the original droop coefficient unchanged. The improved droop characteristic is expressed as:

$$\begin{cases} \omega_i = \omega_{ni} - m_{pi}(P_i - P_{ni}) - \hat{m}_d \dfrac{\mathrm{d}P_i}{\mathrm{d}t} \\ v_{oi}^* = V_{ni} - n_{qi}(Q_i - Q_{ni}) - \hat{n}_d \dfrac{\mathrm{d}Q_i}{\mathrm{d}t} \end{cases} \tag{8}$$

where $\hat{m}_d$ and $\hat{n}_d$ are the respective adaptive transient droop coefficients. The adaptive characteristic also provides active damping for power oscillation in different operating conditions. This improves the stability of the system. Nevertheless, detailed parameters of the power line are required to implement the method. Moreover, a poor design may lead to positive feedback and cause system instability [62].

To improve the stability margin of the system, the method of introducing lead compensators in traditional droop control, also called transient droop control, may be used [12]:

$$\omega_i = \frac{1+sT_{a1}}{1+sT_{b1}} \times \cdots \times \frac{1+sT_{aj}}{1+sT_{bj}} (\omega_{ni} - m_{pi}(P_i - P_{ni})) \tag{9}$$

where T_{a1}, T_{b1}, T_{aj}, and T_{bj} are the time constants of the first and jth lead compensators, respectively. The method can significantly optimize the stability margin of the islanded MG system [11], but the optimization effect will gradually become saturated with the increase of the lead compensators [12]. In addition, the system pole-zero location may be changed by this method, and thus the stability margin of the system needs to be re-evaluated.

In the traditional droop mechanism, the power-sharing dynamic performance of a weak system such as MG can be improved by a large droop factor. However, it is accompanied by a reduction in the damping of the system. This makes the system more susceptible to instabilities. To reduce the dependence of system damping on the droop factor, some studies have added an additional auxiliary loop on the active power loop to correct the voltage reference signal, which can improve the system damping without affecting the active sharing performance [64], [86].

A detailed overview of the existing primary control strategies for AC MG systems is provided in Table I. Adopting corresponding control strategies for specific scenarios can effectively improve the dynamic performance and stability of MGs. Therefore, further improvements and integration of existing primary control strategies in the hierarchical structure will help to improve the design and implementation of future distributed and multi-level AC MG architectures.

B. Secondary Control

In conventional droop control, it is hard to avoid the existence of voltage and frequency deviations between different units because of the absence of necessary communication links [4], [29], [56]. Considering the limited capacity of energy storage devices, secondary control is introduced to recover voltage and frequency by sending compensating reference signals to the primary controller, as shown in Fig. 5, and the droop control strategy after compensation is expressed as [29]:

$$\begin{cases} \omega_i = \omega_{ni} - m_{pi}(P_i - P_{ni}) + \delta u_{\omega,i} \\ v_{oi}^* = V_{ni} - n_{qi}(Q_i - Q_{ni}) + \delta u_{v,i} \end{cases} \tag{10}$$

where $\delta u_{\omega,i}$, and $\delta u_{v,i}$ are the control signals from the secondary control, and the design of these signals is based on data sharing between DGs, such as frequency, voltage, and power information. In Fig. 5, voltage and frequency recovery can be realized through secondary control when the load demand increases [22]. After reaching the steady-state, the frequency of each generator is the same, and the system achieves accurate active power-sharing. In addition, the local nature of the output voltage is also weakened through the prediction of reactive power-sharing [87].

Secondary control is mainly implemented in centralized or distributed ways. In the centralized control architecture, the MGCC needs to receive and process global information from units of the MG and provide control signals to the lower control layers. As more DG units are connected to the system, traditional centralized control will be faced with technical challenges such as communication delay, low reliability, and complex structure [88], [89], hence it is often mainly used in small MGs. On the other hand, when distributed control is adopted, MGCC only processes limited information or no central control, which takes full advantage of the participation and autonomy of units and sparse communication networks to reduce system operating costs and improve system scalability and operational reliability [4], [89], [90]. Distributed secondary control can be achieved through different algorithms, such as the consensus-based algorithm in which each node of the network runs synchronously and updates its current state based on the information provided by neighboring agents [91]. However, distributed control is more demanding on the control algorithms, and its communication network design is also complicated.

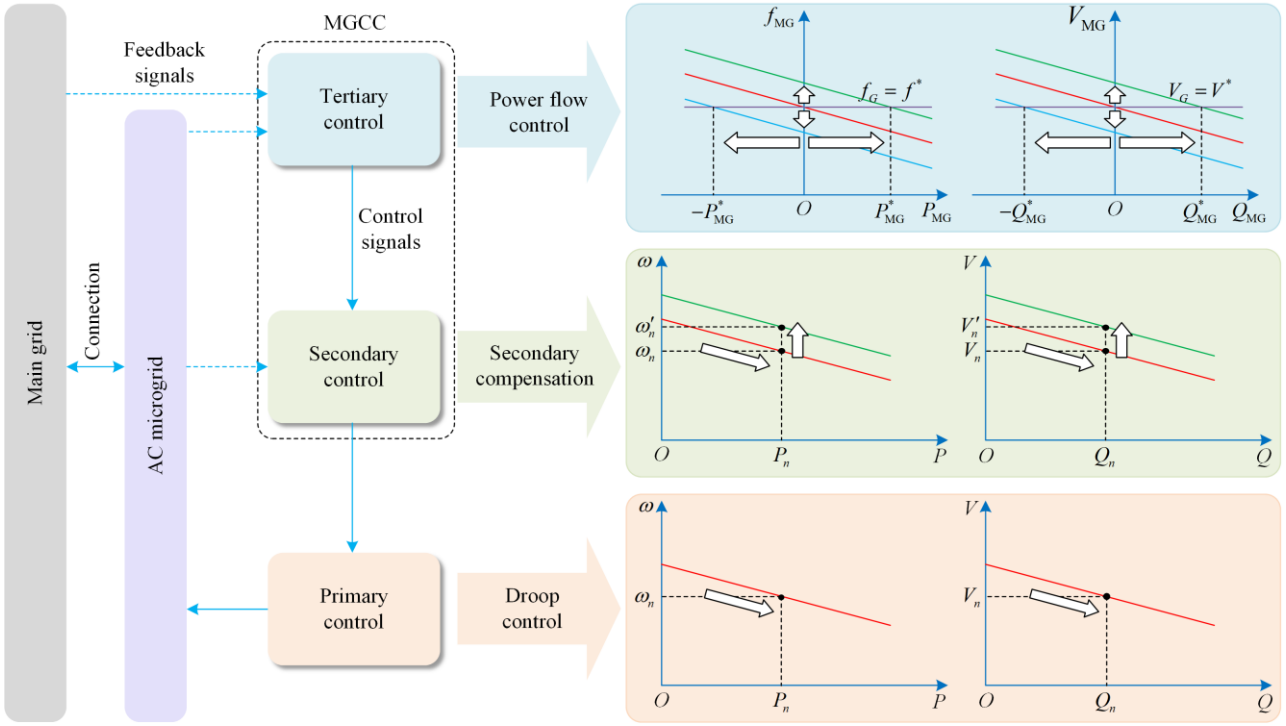

Fig. 5. Response of each control layer in a hierarchical control structure for the microgrid [4], [22].

C. Tertiary Control

Tertiary control is the highest level of control in the current hierarchical control, and its control objectives include power flow control and energy management. The precise power-sharing among DGs and the power exchange between the MG and the main power grid are implemented by power flow control, while the purpose of energy management is to realize long-term economic operation based on energy price and the power market [5]. The control technology used in tertiary control is mostly related to economic aspects [3].

When the MG is connected to the grid, the flow direction of active and reactive power between the MG and the main grid is controlled by tertiary control by adjusting the respective reference value of the MG's frequency and voltage amplitude [22]:

$$\begin{cases} f^*_{\mathrm{MG}} = k_{pP}(P^*_{\mathrm{PCC}} - P_{\mathrm{PCC}}) + k_{iP}\int (P^*_{\mathrm{PCC}} - P_{\mathrm{PCC}})\mathrm{d}t \\ V^*_{\mathrm{MG}} = k_{pQ}(Q^*_{\mathrm{PCC}} - Q_{\mathrm{PCC}}) + k_{iQ}\int (Q^*_{\mathrm{PCC}} - Q_{\mathrm{PCC}})\mathrm{d}t \end{cases} \tag{11}$$

where k_{pP}, k_{iP}, k_{pQ}, and k_{iQ} are the control parameters of the tertiary control; P_{PCC}, P^*_{PCC}, Q_{PCC}, and Q^*_{PCC} are the measured and desired P/Q values at the PCC, respectively; f^*_{MG}, and V^*_{MG} are the frequency and voltage amplitude reference signals of the MG, respectively. These are provided by the secondary control in the islanded mode or the tertiary control in the grid-connected mode. In Fig. 5, the bi-directional power flow between the MG and the main grid can be realized through the tertiary control action. The main grid has constant frequency f_{G} and amplitude V_{G}, and thus the power exchange between the MG and the main grid can be determined by the intersection of the droop characteristic of the MG and the constant feature of the main grid. The active power flow is controlled by adjusting the frequency, e.g., if $f^*_{\mathrm{MG}} > f_{\mathrm{G}}$, then $P^*_{\mathrm{PCC}} > 0$, and the MG injects P to the main grid, while if $f^*_{\mathrm{MG}} < f_{\mathrm{G}}$, then $P^*_{\mathrm{PCC}} < 0$, and the MG absorbs P from the main grid. In the response process, reactive power control is implemented similarly to active power control. The optimization and decision-making functions can be applied in tertiary control to provide the optimum parameters for lower order controllers to realize an intelligent and efficient operation of the whole system [5].

As the last control layer, it is slow in response compared to primary and secondary controls. In traditional hierarchical control, centralized control is commonly used in the secondary and tertiary control [23]. The system is faced with large computation problems, high communication costs, and low reliability and these are caused by centralized control. In Fig. 6, decentralized control is adopted for the primary and secondary controls to reduce the reliance of the system on central control and communication links and to improve the reliability of the system in the case of single point of failure [90]. In addition, the application of distributed control in large MGs based on sparse communication networks and neighbor communication is a viable direction for the control technology in MGs. For large-scale MG and MGC systems, an advanced method

called multi-agent system (MAS)-based control is proposed in [26] as tertiary control. This divides the large-scale system into several autonomous and mutually communicating agents to realize information sharing and coordinated control of the system in the distributed environment. A three-layer MAS structure is built in [88] to realize flexible, coordinated control of the MGC system through the cooperation of agents. However, the control architecture is not as efficient as grid-connected operation during islanded operation [90], and the dynamic performance of the system is also affected by the potential uncertainties of communication such as latency and packet loss [89].

As a global control, tertiary control can be considered part of the main grid rather than only belonging to the MG. The synchronization and reconnection between the MG and the main grid are based on the collaboration of tertiary and secondary control [5]. To ensure the stability of the voltage and frequency of the system in an unscheduled intentional island, tertiary control will be disabled by MG, and thus, an island detection algorithm is necessary [22].

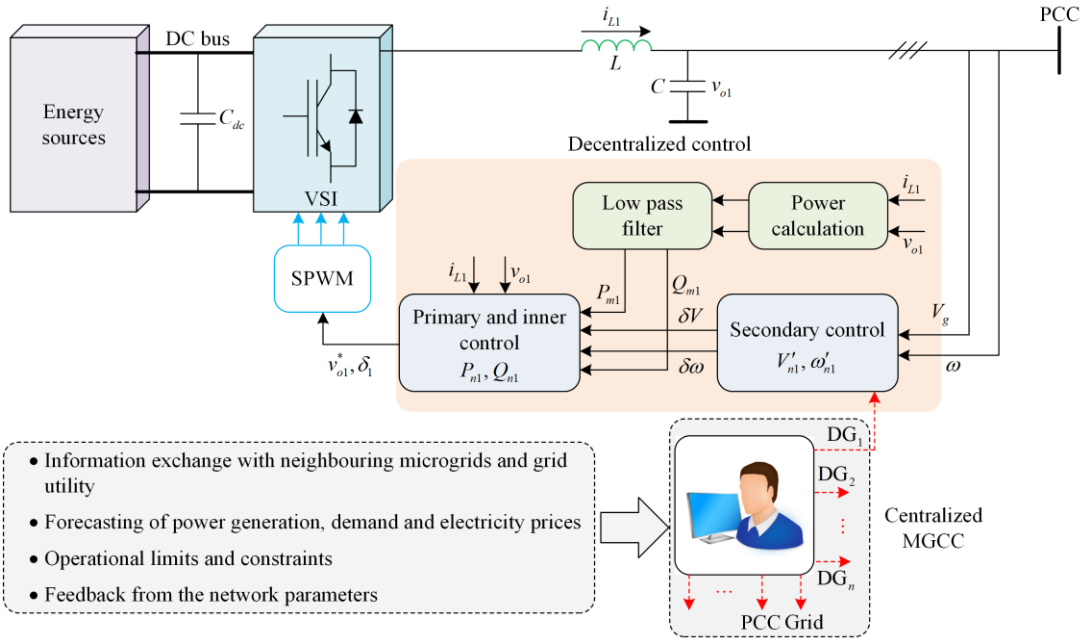

Fig. 6. Centralized and decentralized controls of the microgrid [90].

With the increase in the number of DGs and network scales, as well as the introduction of equipment with non-stationary dynamic characteristics, MGs face great challenges in energy service and protection, and hierarchical control techniques that can coordinate energy exchange between MGs or MGCs have good application prospects. However, in design or optimization, the mathematical model of the system will become very complex, while multi-timescale features are prominent, making stability analysis and optimization of the system difficult. An overview of the existing modeling and simplification approaches applicable to MG systems from a timescale perspective is provided in the following sections.

III. Multi-timescale Modeling of AC MG

Considering the special dynamic nature of an MG, multi-timescale coupling models are required for system analysis. This poses new challenges to the accuracy and computational efficiency in the system modeling and analysis [92]. Currently, different typical modeling methods are suitable for specific scenarios, e.g., some models are suitable for small-signal stability analysis, and others are suitable for simulation and global stability analysis. This section presents several modeling approaches commonly used in large- and small-signal stability analyses, and their applicability is compared. Directly building models with all the features for complex objects often faces problems such as difficulty in modeling, low computational efficiency, and poor scalability. Therefore, the corresponding model simplification methods are also presented.

A. Small-signal Modeling

Small-signal models are essential for small-signal stability analysis and linear controller design of MG systems [18], [35]. Considering the multi-timescale nature of MG systems, the dynamics of each component need to be fully addressed for an accurate small-signal model [18]. In addition, the preservation of nonlinear coupling characteristics is also critical to the study of dynamic interaction problems.

Currently, small-signal stability analysis methods for power-electronized power systems mainly include eigenvalue analysis and impedance analysis, and the small-signal models used in these methods are the state-space model and the impedance model, respectively [61], [93].

1) State-space Model

The state-space methods are typical small-signal modeling methods using small-signal linearization, which refers to approximating a nonlinear system around a given operating point or a trajectory with small-signal perturbations [38]. In general, after a small-signal linearization process, a linear time-invariant (LTI) state-space model of the power system can be derived from the nonlinear differential equations, as [40]:

$$\Delta\dot{x} = \boldsymbol{A}\Delta x + \boldsymbol{B}\Delta u \tag{12}$$

where $\boldsymbol{A}$ and $\boldsymbol{B}$ are the time-invariant state matrix and input matrix for the LTI system, respectively; while Δx and Δu are small perturbations of state variables and input variables, respectively. To establish the state-space model of the MG system, the common modeling method first divides the global system into several subsystems, including DGs, networks, and loads. Each subsystem is modeled based on the local reference frame. Before integrating the global dynamic model, all units need to be translated into a common reference frame using transformation techniques [81]. It is worth noting that the state-space model depends on the integrity and certainty of the system. Once the structure or parameters of the system change, the state-space model needs to be rebuilt. However, the parameters of the MG units, such as loads, are difficult to determine in practice [34].

Considering the impact of power electronic converters on system stability, an accurate converter model is critical to the global model. In fact, converters are nonlinear time-varying dynamic systems that contain both continuous dynamics of passive components and discrete dynamics of switching devices [36]. The continuous dynamic model modeling methods of the converter include: 1) state-space averaging; 2) generalized averaging; and 3) the harmonic state-space (HSS) method.

a) State-space Averaging Model

This method is typical for obtaining continuous dynamics models of converters. The basic idea of the method is to filter out the switching waves for a switching period by the following moving average operator [36].

$$\bar{x}(t) = \frac{1}{T_s}\int_{t-T_s}^{t} x(\tau)\mathrm{d}\tau \tag{13}$$

where T_s is the switching period of the converter. Applying the averaging method to the switching model, the averaged model can be represented in a general form as [32]:

$$\frac{\mathrm{d}\bar{x}(t)}{\mathrm{d}t} = (\sum_{k=1}^{N} d_k \times \boldsymbol{A}_k) \times \bar{x}(t) + (\sum_{k=1}^{N} d_k \times \boldsymbol{B}_k) \times \bar{u}(t) \tag{14}$$

where d_k is the duty ratio of equivalent circuit k; and $\boldsymbol{A}_k$ and $\boldsymbol{B}_k$ are the system matrices corresponding to the kth circuit. The averaged models obtained by this method are still nonlinear and time-varying, and need to be further linearized [36]. The effect of this method is equivalent to a low-pass filter. It is difficult to ensure the accuracy of the models at high frequency [38]. Therefore, it is only applicable to the stability analysis of the slow timescales [35]. It is also difficult for this method to reflect the harmonics and their interactions in the electromagnetic transient processes of three-phase unbalanced systems [37], [38].

b) Generalized Averaging Model

To cope with the research needs of frequency-coupled unbalanced systems, this method considers the effects of the high and low-frequency components of state variables. It is worth noting that, considering the dominance of low-frequency stability, the involvement of low-frequency components is emphasized when reconstructing the state variable operator. If the periodic signal is absolutely integrable within a period, the operator can be expressed as [37]:

$$x(t) = \sum_{k=-\infty}^{\infty} \langle x \rangle_k (t) \mathrm{e}^{\mathrm{j}\omega_s t} \tag{15}$$

where ω_s is the switching frequency of the converter; $\langle x \rangle_k$ is the k-order Fourier coefficient of $x(t)$, also known as the k-order dynamic phasor, and is defined as [36]:

$$\langle x \rangle_k (t) = \frac{1}{T_s}\int_{t-T_s}^{t} x(\tau)\mathrm{e}^{-\mathrm{j}k\omega_s T_s}\mathrm{d}\tau \tag{16}$$

Based on the differential and convolution properties of the Fourier transform, the generalized averaging model of the converter is established in terms of real and imaginary parts of the order required by the state variables [37]:

$$\frac{\mathrm{d}}{\mathrm{d}t}\langle x \rangle_k (t) = \langle f(x(t),u(t)) \rangle_k (t) - \mathrm{j}k\omega\langle x \rangle_k (t) \tag{17}$$

Compared with the state-space averaging model, the dynamic phasor model in the dq-frame is time-invariant. As a multi-frequency model, the generalized averaging model is suitable for global stability analysis and can be extended to single-phase and unbalanced three-phase systems. The cross-coupling between the order components can be reflected by the convolution property of the Fourier transform [36]. However, this model cannot predict the frequency-coupled interactions between converters [38]. The accuracy of the generalized averaging model is between the quasi-steady model and the detailed model. This depends on the components used to construct the state variables and the switching period [37]. When the number of the components considered is small, a harmonic truncation error will occur, and the accuracy cannot be guaranteed when the harmonic components and the proportion are large [39].

c) HSS Model

When the power system contains time-varying elements, a linear time-periodic (LTP) model can be obtained by linearization, which is given by [36]:

$$\Delta\dot{x}(t) = \boldsymbol{A}(t)\Delta x(t) + \boldsymbol{B}(t)\Delta u(t) \tag{18}$$

where $\boldsymbol{A}(t)$ and $\boldsymbol{B}(t)$ are time-periodic matrices. Based on the LTP system theory and the HSS method, the HSS model can be derived from the LTP model [38]. Unlike the operator generated by the generalized averaging method, the state variables in the HSS model given below are represented by the sum of the components in the frequency domain, and an exponential modulation periodic function is introduced to describe its transient process [36], [38], [40].

$$x(t)=\sum_k x_k(t)\mathrm{e}^{\mathrm{j}k\omega_s t}=\mathrm{e}^{st}\sum_k X_k(s)\mathrm{e}^{\mathrm{j}k\omega_s t} \tag{19}$$

where $s=\sigma+j\omega$ is used to modulate the Fourier coefficients for extracting the transient responses of harmonic components. These coefficient matrices of the system are also replaced by the Fourier series [36], [38], e.g.:

$$\boldsymbol{A}(t)=\sum_k \boldsymbol{A}_k\mathrm{e}^{\mathrm{j}k\omega_s t} \tag{20}$$

By substituting for $\Delta x(t)$ and $\Delta u(t)$ by their respective forms in (19), the HSS model is obtained as:

$$(s+\mathrm{j}k\omega_s)X_k(s)=\sum_n \boldsymbol{A}_{k-n}X_n(s)+\sum_n \boldsymbol{B}_{k-n}U_n(s) \tag{21}$$

In this way the LTP system is represented by a multi-frequency state-space model containing multiple inputs and outputs. Unlike the generalized averaging model, the linearization of the HSS model is more direct, and its coefficient matrices and signals are expressed by the amplitude and phase angle constants of each frequency in the complex frequency domain [40], [41]. However, the HSS model usually has a high order because multiple frequency components are involved in the modeling process [38].

2) Impedance Model

Based on a certain point, the impedance analysis divides the whole system into two independent subsystems, including the source subsystem and the load subsystem, which are represented by a Thevenin or Norton equivalent circuit [61], [75], [93]. Unlike the state-space model, the impedance model can be obtained from measurements in addition to calculations, and thus it is less dependent on detailed parameters [34]. Moreover, each subsystem is modeled independently and without interfering with each other. Therefore, it is not necessary to reconstruct the impedance model when the structure and parameters of any other party change. This significantly reduces the modeling workload.

In the process of building the impedance model of the grid-tied inverter, if the PCC is taken as the reference point, and the small-signal of the PCC voltage Δu_{PCC} and the grid-tied current Δi_g are considered as the excitation and response, then the transfer function of the inverter's admittance $\boldsymbol{Y}_i$ can be obtained through the equivalent transformation of the control block diagram. Calculating the inverse matrix of $\boldsymbol{Y}_i$, the inverter equivalent output impedance $\boldsymbol{Z}_i$ can be obtained as [93]:

$$\boldsymbol{Z}_i(s)=\boldsymbol{Y}_i^{-1}(s) \tag{22}$$

The impedance analysis requires that the object of study is LTI while the AC MG system is nonlinear time-varying. Hence, two feasible impedance modeling methods, the linearization method in the *dq*-frame and the harmonic linearization modeling method have been proposed [34]. The former method models the impedance of the converter in the *dq*-frame, which corresponds to the control system based on the same frame. However, there are some couplings between the *d*-axis and *q*-axis structures in the AC three-phase system [34], [93]. Therefore, the non-zero non-diagonal elements in the impedance matrix cannot easily be ignored, which makes the stability analysis of grid-connected inverters more complicated. The latter method obtains the system impedance model based on the response results of adding harmonic interference signals at different frequencies to the excitation [94], [95]. In this method, the symmetrical components method is adopted, and the system is decomposed into positive and negative sequence subsystems. It is worth noting that the obtained sequence impedance is usually decoupled and has a clear physical definition. Therefore, this method can also be used for impedance modeling of three-phase unbalanced or single-phase systems. However, the complex phase sequence transformation and algebraic operations based on the circuit structure increase the complexity of the modeling.

B. Large-signal Modeling

Since the validity of linearization can only be guaranteed around the steady-state operating point, small-signal models can only be applied to quasi-steady-state analysis [3], [46], [78]. Therefore, it is necessary to develop standard nonlinear models to reflect the transient characteristics of the system. Two modeling approaches suitable for large-signal stability analysis are reviewed below: piecewise linear models and discrete-time models.

1) Piecewise Linear Model

The piecewise linear model is based on the state-space averaging model, and its core is to decompose the simulation time into reasonable subintervals, within which the state equation of the converter is averaged instead of a single switching period [36]. Hence, in each subinterval, the converter model is linear, expressed as [32], [35]:

$$\frac{\mathrm{d}x(t)}{\mathrm{d}t}=\boldsymbol{A}_k x(t)+\boldsymbol{b}_k, x(t)\in X_k \tag{23}$$

where X_k is a region of the state space, $\boldsymbol{A}_k$ and $\boldsymbol{b}_k$ correspond to the system matrices of the k circuit topology. $k\in K, K=\{1,\cdots,m\}$, $X_1\bigcup X_2\cdots\bigcup X_n=X, X\subseteq R^n$. To simulate the transient process accurately, the simulation step size is set to one-tenth of the switching period or less. This is more accurate than the state-space averaging model, and it can be used to analyze the fast-timescale stability of power electronics converters. However, there is no strict basis for the segmentation of simulation time,

and the errors and ripples caused by the timescale expansion need to be considered separately [37].

2) Discrete-time Model

The discrete-time model is also called the sampling data model. For simplification, the sampling period is assumed to be equal to the switching period, and the functional relationship between the sampling points is obtained by integration and derivation. Then, by linearizing the function, the corresponding sampling data model is obtained. This can be expressed as:

$$X^{(n+1)} = f(X^{(n)}, d, U) \tag{24}$$

where $X^{(n)}$ is the state of $t = nT$; T is the sampling period; and $d = \left[d_1, d_2, \cdots, d_n\right]^T$. In most practical applications, the modeling of converters is based on the continuous-time averaging method. However, this method not only ignores the nonlinear characteristics of converters, such as the bifurcation phenomenon in the approximation process, but also fails to accurately study the control delay inherent in the digital control systems. Also, the continuous-time model cannot predict the fast-scale dynamics associated with the switching operation of the system. For the problems presented above, the discrete-time model has obvious advantages [97]. However, because of the influence of the discretization methods, the mapping from *s*-domain to *z*-domain can introduce some discrepancies, leading to inaccurate prediction of the dynamic characteristics, and it is difficult to compare the design results with the experimental results [32], [96]. In addition, sampling, modulator effects, and delays in the control loop are important factors affecting the accuracy of the discrete-time model [98].

The piecewise linear model and the discrete-time model are both accurate models and suitable for slow- and fast-scale stability analysis [35]. However, these modeling approaches are not entirely compatible, especially as the scenario expands to the whole system level. Table II summarizes the comparative results between various large-signal and small-signal modeling methods.

TABLE II
COMPARISON OF LARGE- AND SMALL-SIGNAL MODELING METHODS FOR A MICROGRID

	Models	Accuracy	Efficiency	Complexity	Effective timescale	Application	Limitations
State-space models	State-space averaging models [35], [36], [38]	Medium	High	Simple	Slow-scale	Three-phase balanced systems	Sideband effects, harmonics, and their interactions are not considered
	Generalized averaging models [37], [39]	Medium~ High	Low~ High	Simple~ Complex	Fast-scale and slow-scale	Multi-frequency coupling	Not suitable for signals containing amount of harmonic components; Harmonic truncation error
	HSS models [40], [41]	High	Low	Complex	Fast-scale and slow-scale	Multi-frequency coupling	The spectrum leakage caused by the Fourier transform
	Piecewise linear models [37]	High	Low	Complex	Fast-scale and slow-scale	Device and subsystem levels	Lack of subsection basis; The error caused by ripple and extended timescale is not considered
	Discrete-time models [94]–[96]	High	Low	Complex	Fast-scale and slow-scale	Device and subsystem levels	The spectrum leakage caused by sampling period setting
	Impedance models [34], [93]–[96]	High	High	Simple	Slow-scale	Multi-converter paralleling systems	The internal stability of the converter cannot be analyzed

C. Model Simplification

The stability analysis at the device level is widely used in parameter design, and detailed models with high precision can be adopted without considering scalability. However, when the stability analysis is extended to the multi-DG system, the scalability and computational efficiency of the model become important. On the other hand, because of the nonlinear coupled structure of the system, it is also very difficult to gain insight into the key factors affecting stability through detailed models [99]. Thus, there are growing appeals for reliable ROMs that retain the main dynamic behavior of the system.

To simplify the stability analysis, previous AC MG modeling has often been based on assumptions such as ignoring the dynamics of the DC side [6], [80], [81] and the internal loop control [100], [101] of the inverters. However, this would lead to critical dynamics being ignored for large capacity inverters, since their low switching frequency limits the bandwidth of internal control loops [82]. Therefore, simplified models need to retain the dominant dynamics to ensure accuracy. The widely used methods for simplifying models of power-electronized power systems are reviewed, including dynamic aggregation and order reduction based on singular perturbation theory [35]. In addition, the equivalent methods for network models and the simplified methods for impedance models are presented.

1) Dynamic Aggregation

The MG system integrates a large amount of equipment for renewable energy, and contains many units with low capacity. With the increase in system size, it is not realistic to include every device in modeling. Consequently, the generator sets need be clustered, and all of the dynamic characteristics of each category are expressed by one or a few equivalent models [35]. A model-reduction method based on dynamic aggregation is proposed in [102], where inverters are clustered based on their electrical distance from the grid, and the

equivalent model of each clustering is derived. The model simplification of loads, especially constant power load (CPL) models, is also an important development direction for this method. An overview of research on the purpose, application scenarios, and aggregation methods of demand-side load aggregation is presented in [103]. However, the method is unable to analyze the effects of factors such as changes in individual device parameters, and the complex dynamic behavior of devices can make equivalent aggregation difficult. In addition, there is a lack of unified, concise, and effective equivalence criteria for equipment such as grid-connected inverters.

2) Singular Perturbation Reduction

Based on the multi-timescale characteristics of the MG system, variables can be divided into fast and slow variables according to the timescale [104]. After decoupling variables with different timescales, fast variables are ignored, and slow variables are retained to achieve model order reduction. The order-reduction process of the state-space model based on singular perturbation theory is:

Step 1: Obtaining the full-order state-space model of the system. First, eigenvalues and eigenvectors of the state matrix are calculated to identify the dominant modes of the system. Then, through the participation factors analysis below, the influencing degree of each eigenvalue on the mode is ascertained [83]:

$$p_{ij} = \frac{\left|u_{ij}^T\right|\left|v_{ij}\right|}{\sum_{k=1}^{N}\left|u_{kj}^T\right|\left|v_{jk}\right|} \tag{25}$$

where i is the number of modes; and j is the number of state variables.

Step 2: Obtaining the perturbed model of the system. Based on the results of the participation factor analysis, all state variables of the system are classified into slow variables (having significant effects on the dominant modes) and fast variables (having little impact on the dominant modes). Then, the state equations related to fast variables are changed to the following perturbed form, while the original state equations of slow variables are retained, i.e.:

$$(\sum_{\varepsilon})\begin{cases}\dfrac{\mathrm{d}x}{\mathrm{d}t} = f(x,z)\\ \varepsilon\dfrac{\mathrm{d}z}{\mathrm{d}t} = g(x,z)\end{cases} \tag{26}$$

where $\varepsilon > 0$ is a small real number; while $x \in R^n$ and $z \in R^m$ are slow and fast variables of the system, respectively.

Step 3: Setting $\varepsilon = 0$, the state equations in the singularly perturbed form can be converted into the steady-state equations, as:

$$g(x,z) = 0 \tag{27}$$

Also, the steady-state solution of fast variable z can be derived as:

$$z = h(x) \tag{28}$$

Finally, by substituting (27) and (28) into (26), the original (n+m)-order system model can be simplified to n-order, given by:

$$\dot{x} = f(x, h(x)) \tag{29}$$

Based on the participation factor analysis, the perturbed ROM can accurately describe the dominant dynamic features in the system. However, because of the linearization nature of the model, the participation factor can only give an accurate correlation between the low-frequency mode and the state variables [108]. Therefore, the contribution of state variables to global modes of the system under actual transient perturbations is still to be further investigated.

3) Kron Reduction

Kron reduction is a method to simplify the dynamic model of the electrical network. It assumes that network nodes are classified either as internal or boundary nodes. After that, the complex network model is replaced by a simpler circuit having fewer nodes but the same terminal behavior of voltages and currents at target vertices [106], [107]. ROM is used to analyze the oscillations between inverters in [82]. To account for the general case of inverters with coupling inductors, the Kron reduction method is involved in this model to present a simplified topology that allows inter-inverter oscillating currents to be singled out. Finally, a small-signal model is derived based on singular perturbation theory.

The Kron reduction is suitable not only for the model simplification of steady-state networks but also for transient stability analysis [82], [106]. In [105], model-reduction methods are proposed for systematically reducing large-signal dynamic models of droop-controlled inverters in islanded MGs, where Kron reduction is employed to isolate the mutual inverter interactions and clearly illustrate the equivalent loads that the inverters have to support in the MG. In applying Kron reduction for transient analysis, admittance models of the network are replaced by differential models, so it is difficult to ensure that the simplified circuit has the same structure of transfer functions as the original model [106].

4) Other Methods

In the modeling of impedance models for inverters, a large number of inverse operations are needed to derive the impedance matrix in (22), which contains coupling terms that make it difficult to establish a connection with the actual physical parts. In [93], the coupling terms of the impedance matrix are divided into two categories according to their correlation with the PLL. Considering the effect of the dynamic error of the PLL, the coupling terms introduced by the PLL are retained, while the coupling terms introduced by other parts are ignored to simplify the impedance model. Also, the obtained impedance expression has a clear relation with the actual physical parts, which is helpful when determining theoretically the influence of the stable op-

eration points and control parameters on the inverter impedance. In classifying the coupling terms, the method, similar to participation factors analysis, essentially refers to the concept of sensitivity analysis.

The advantages, disadvantages, and applicability of the various model simplification methods applied to the multi-timescale model of the MG are summarized in Table III.

TABLE III
ADVANTAGES, DISADVANTAGES, AND APPLICATION OF MODEL SIMPLIFICATION METHODS IN MICROGRID

Methods	Advantages	Disadvantages	Application
Dynamic aggregation [35], [100], [101]	√ Integrate a large number of generation-side/demand-side units into a flexible aggregator that participates in system dispatching	× The effects of randomness and intermittency of individual equipment on the global model are ignored	◆ Fast-scale and slow-scale ◆ Large number of generation-side units or demand-side loads
Participation factors analysis [81], [102]	√ Reflect the degree of influence of parameter changes on system state variables √ Identify key parameters that affect the stability of the system at low frequencies.	× Perturbation aspects are not taken into account when analyzing the contribution of the model to the state variables	◆ Low-frequency oscillation analysis ◆ Design of power system stabilizers
Singular perturbation reduction [77], [81], [102], [103]	√ Simplify the model of the system in terms of timescales √ Retain the main dynamic features of the system	× The basis for classifying fast and slow variables will affect the accuracy of the model	◆ Fast-scale and slow-scale ◆ Reduction of higher-order models with multiple timescales
Kron reduction [80], [103]–[105]	√ Retain the characteristics of the network target node √ Interactions between components can be separated	× The simplified circuit structure would be changed	◆ Fast-scale and slow-scale ◆ Complex network model simplification

IV. MULTI-TIMESCALE DYNAMIC STABILITY ANALYSIS OF AC MG

A. Definition and Classification of Multi-timescale Dynamic Stability in the MG

1) Definition

The dynamic stability of an MG refers to the ability to restore stable operation after disturbances, relying on control measures such as control loops, energy storage devices, and generator/load shedding. This is a collection of dynamic characteristics on different timescales like power equipment and networks [63]. In traditional power systems, synchronous generators are the biggest factor that affects the dynamic performance of the system [33]. However, DGs in MG systems are generally connected to the grid through inverters, which leads to inertia defects [73]. These inverters may also adopt different control strategies, making the system heterogeneous and prone to stability problems [11]. In the hierarchical control strategy, there are some inherent communication delays in the processes of information acquisition and transmission, and even packet dropout, which can lead to system instability [1], [109]. The introduction of multi-timescale controllers in power electronics equipment broadens the frequency bandwidth of the system [32], and the equipment also responds to disturbances within the broadband [33]. The MG is anonlinear system in nature, which leads to dynamic coupling and interactions between components with different timescales [35]. For example, the electromagnetic delay of the network, despite having sufficiently fast timescale dynamics, can affect the dynamic behavior of the degrees of freedom associated with slower timescale droop control [99]. In multi-inverter paralleling systems, there are interactions between inverters and the power grid. They cause harmonic resonances and system instability [75]. There are also dynamic interactions between sources and loads. These increase the complexity of the dynamic stability analysis in the MG system. With the increase in system size and capacity, the interactions between components become more noticeable [6], [34]. To further investigate the mechanisms and characteristics of MG systems, the classification of system dynamic stability needs to be reconsidered.

2) Classification

As a smaller low-voltage distribution system, an MG has a small and predominantly resistive line impedance, which leads to small phase angle differences between the node voltages [22]. Therefore, more attention is paid to the stability of voltage and frequency in the stable operation of the MG system. On the one hand, MG voltage stability refers to keeping the voltage amplitude at the levels required by the system [110]. Different from the frequency, the voltage is a local variable, and there is a circulating reactive current between DGs [60]. Under normal line conditions, the coupling of voltage control and active power control is significant [4], [11], [22]. Typical problems, such as inaccurate reactive power-sharing in classical droop control, are caused by the difference in the line impedances between the inverters and the PCC [22]. The dynamic characteristics of the loads also affect the voltage and transient stability of the MG [110]. With the large-scale use of new energy sources, the short-circuit capacity of the system decreases significantly, and the main grid has insufficient capacity to support the voltage. System flows also fluctuate dramatically because of the characteristics of

the new energy sources, significantly increasing the voltage regulation pressure on the system.

On the other hand, the frequency stability of an MG refers to the system frequency within the preset limits. In grid-connected mode, frequency is regulated by the main grid as a global variable [90]. However, in islanded operation, MGs need to control system frequency through coordination and synchronization between various units in the system [110]. With conventional generators being replaced by the new energy sources in the MG, the frequency regulation capacity of the system is significantly reduced. In the classical droop control mechanism without communication, which is widely used in the MG system, it leads to voltage and frequency deviations [22], [29], [111], [112], and the design of the droop coefficient also needs to consider the balance between power-sharing and system stability [22], [25], [45], [58], [113]. In addition, because of the strong nonlinear characteristics, the voltage and frequency of the MG are coupled, and it is difficult to simply classify the instability phenomenon of the system as the instability of voltage and frequency [3].

The voltage and frequency stability of the MG can be determined by small- and large-signal stability analysis [90]. The asymptotic stability of the system at the operating point can be determined based on the linearized model through small-signal stability analysis, but information on the stability margin at the operating point cannot be provided [114]. This problem can be overcome by implementing large-signal stability analyses based on non-linear techniques. However, compared with the traditional power system, the MG system has more complex dynamic characteristics, and there are interactions between power electronic equipment, power networks, and generator mechanical motion. These may lead to unstable oscillations in the power system over a wide frequency range. To accommodate this change, based on singular perturbation and stability region theory, a timescale decomposition method for power system stability analysis is proposed in [47], [51], [53]. This establishes a link between the traditional large- and small-signal stability analysis, and is applicable to the analysis of multi-timescale systems.

In MG systems, the main factors causing small disturbances include feedback controllers, load changes, power limitations of DGs, and communication delays, while the main factors causing large disturbances include system faults, mode switching, and DG/ load switching. For the above factors, there are various ways to improve the stability of the MG, such as through auxiliary controls of DGs [12], [30], [64], [75], stabilizers [115], coordinated controls [26], [66], [86], and energy storage systems (ESS) [87], 108] to improve the small-signal stability, and the improvement of transient stability is mainly considered from the aspects of ESS, load shedding [116] and transient stability assessments [45]. The stability problems associated with power electronic devices can be divided into slow-interaction stability and fast-interaction stability. Here, the slow interaction mainly refers to the coupling between the control of power electronic equipment and the slow response components of the power system, such as synchronous generators, and the instability is mainly in the form of low-frequency oscillations. For fast interaction, it mainly refers to the coupling between the power electronic equipment control, and power system fast response components, and instability is mainly shown as resonance and high-frequency oscillations caused by interactions between controllers and passive components. Therefore, a study of the interactions and the coupling properties of power-electronized power systems is required to optimize the interaction stability of the system. Based on the above discussions, the dynamic stability classification of an MG is given in Fig. 7 according to relevant variables, instability factors, analysis methods, and optimization.

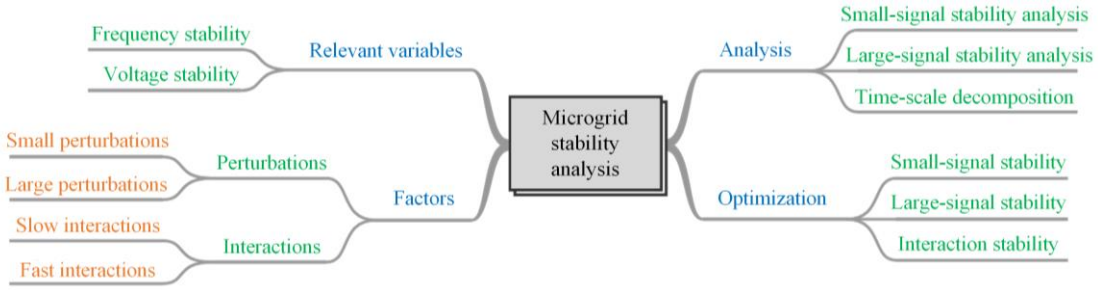

Fig. 7. Dynamic stability classification of the AC MG [1], [3], [88], [114].

B. Multi-timescale Stability Analysis Methods for the MG

1) Small-signal Stability Analysis

MGs are always subjected to small disturbances, such as small output fluctuations in DGs, load changes, parameter variations, etc. In a large-scale power system with large inertia and infinite bus, it is difficult for small perturbations to have a substantial influence on the current operational state of the system. In contrast, MG systems have smaller capacity and lower inertia, while power electronics equipment may introduce negative damping to the power system in various frequency ranges, making the system less stable and weakening the anti-disturbance capability of the system [118]. As the system damping decreases, dynamic interactions become more prominent, and may eventually lead to wide-frequency domain oscillations [82].

The existing studies on the small-signal stability in MGs mainly evaluate the asymptotic stability of the system at a certain equilibrium point. This can provide a certain basis for the design and optimization of system parameters [35], [78]. The small-signal stability analysis of the MG mainly includes eigenvalue analysis methods based on state-space models and impedance analysis methods based on frequency domain criteria [63].

a) Eigenvalue Analysis Method

The eigenvalue analysis method is widely used in electromechanical oscillation analysis in power systems because of its simple principles and strict criteria. This method can identify important information about system stability, such as the system oscillation frequency, oscillation amplitude, and system damping according to the eigenvalue analysis, and provide the basis for system parameter design/optimization combined with the sensitivity analysis. The application processes and steps of this method in small-signal stability analysis of AC MGs are described in detail in [81], involving the modeling of the state-space model, eigenvalue analysis, and sensitivity analysis.

Sensitivity analysis is widely used in stability analysis and parameter design for conventional power systems and MGs because it can reflect how parameter changes affect system state variables [63]. For example, most power electronic loads in MGs behave as CPLs with negative damping characteristics, as shown in Fig. 8, which make the system more susceptible to oscillations [6], [119]–[121]. Based on the linearization theory at operating points, some researchers have developed state-space models for MGs with CPL and analyzed the small-signal stability of the system using eigenvalue analysis [6], [77], [122]–[125]. Moreover, the results of the sensitivity analysis show that CPL has a negative impact on the low-frequency mode stability of the system.

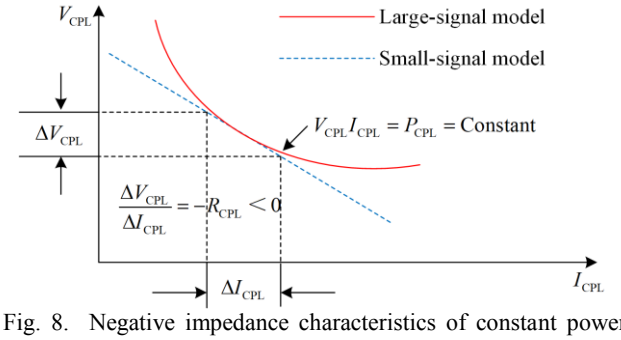

Fig. 8. Negative impedance characteristics of constant power load [116].

As a global stability analysis method, eigenvalue analysis can evaluate the stability of the MG regardless of the location of instability sources [42]. However, this method requires the parameters of all components in the system, and the order of the state-space model at the system level is generally high, which leads to computational difficulties and poor practicability [80]. In addition, the AC MG system is generally unbalanced in the three phases, and the state-space model will become quite complex, which further reduces the practicability of this method [3].

b) Impedance Analysis Method

Based on the concepts of frequency domain transfer functions and impedances, the whole system is divided into load and source subsystems based on a certain node to study the port characteristics of the subsystem [80]. The small-signal stability of the interactive system can be determined when both the source and load subsystems can independently operate stably, and the output impedances of the two subsystems satisfy the Nyquist criterion in the full-frequency band. A review of the impedance modeling and stability analysis methods for grid-connected inverters is presented in [34]. Compared to the eigenvalue analysis, impedance analysis is more feasible in the absence of source and load parameters.

Specific application scenarios for impedance analysis include [42]: ①the interaction stability between the inverter and grid; and ② the interaction stability between multiple inverters. It should be noted that the stability analysis results of this method may change with the variations of nodes, and thus the conclusions are partial and insufficient. The impedance analysis method does not combine with the method similar to the participation factors analysis, and it is difficult to explore the rule that the damping level affects the oscillation modes at present. In addition, when the impedance includes poles on the right-half plane, the accuracy of the stability assessment based on impedance analysis methods may not be guaranteed. Moreover, as a small-signal stability analysis method, this method cannot reflect the stability margin of the system.

2) Large-signal Stability Analysis

Similar to traditional power systems, MG systems suffer from transient instabilities under large perturbations, but because of strong nonlinearities, the interactions within the system are more complex, and the instabilities are often intertwined and difficult to distinguish, which results in more diverse forms of system instability. For power-electronized power systems such as MGs, an important goal of transient stability analysis is to provide system stability margin information to ensure the safe and stable operation of the system [35]. However, small-signal stability analyses are only effective near the equilibrium point of the system and cannot predict or quantify the asymptotic stability domain of the system [35], [78], [90]. Moreover, MGs are nonlinear system in nature, and the small-signal stability analysis methods based on the linear models do not apply to large-signal stability analysis [45]. However, this can be overcome by large-signal stability analysis, and the common methods include time-domain simulation methods and direct methods [3], [126].

a) Time-domain Simulation Method

Time-domain simulation is a mature and widely used stability analysis method. In this method, the curves of the state variables varying with time are obtained by

solving the differential-algebraic equations of the system. In [31], the transient instability process of the asynchronous generator with different mechanical loads is analyzed, and the influence of asynchronous generator parameters on the fault clearing time is validated with simulations performed in the PSCAD-EMTDC environment. In the study on a droop-controlled DC/AC inverter connected to an infinite bus, a methodology is provided in [127] to study the effect of model order reduction on the domain of attraction (DOA) estimation and time-domain simulations. However, the DC-side dynamics and nonlinear characteristics of the inverter are not considered in the modeling process.

Compared with the direct methods, the time-domain simulation methods have higher precision and effectiveness [3]. As the most reliable method for stability evaluations, the time-domain simulation method is suitable for any complex system or control strategy and is often used as the test standard for other transient stability analysis methods. However, the numerical integration of dynamic equations in time domain simulations is slow. With the increase of the order of system state variables, the computation will increase greatly, and the calculation speed cannot meet the demand of online monitoring and control. When the running state of the system changes, the simulation model also needs to be constantly updated. Moreover, the method cannot reflect the quantitative information of the system stability margin and the mechanism of system instability.

b) Direct Method

The direct method, also known as the energy function method, calculates and compares the transient- and critical-energy of the system to assess the transient stability of the system by building a positive definite energy function that has a negative definite derivative. At present, the direct method is mainly used to estimate DOA at the level of power electronics devices and to analyze the mechanism at the subsystem level [35]. For instance, to avoid linearization limitations, some have developed nonlinear state-space models for CPL and performed system transient analysis based on Lyapunov theory [120], [121], [128]–[130]. The basic steps of large-signal system stability analysis are shown in Fig. 9. As seen, after determining the small-signal stability, the large-signal stability of the system can be further evaluated. In addition, the evaluation process mainly consists of two steps: construction of Lyapunov function and estimation of DOA.

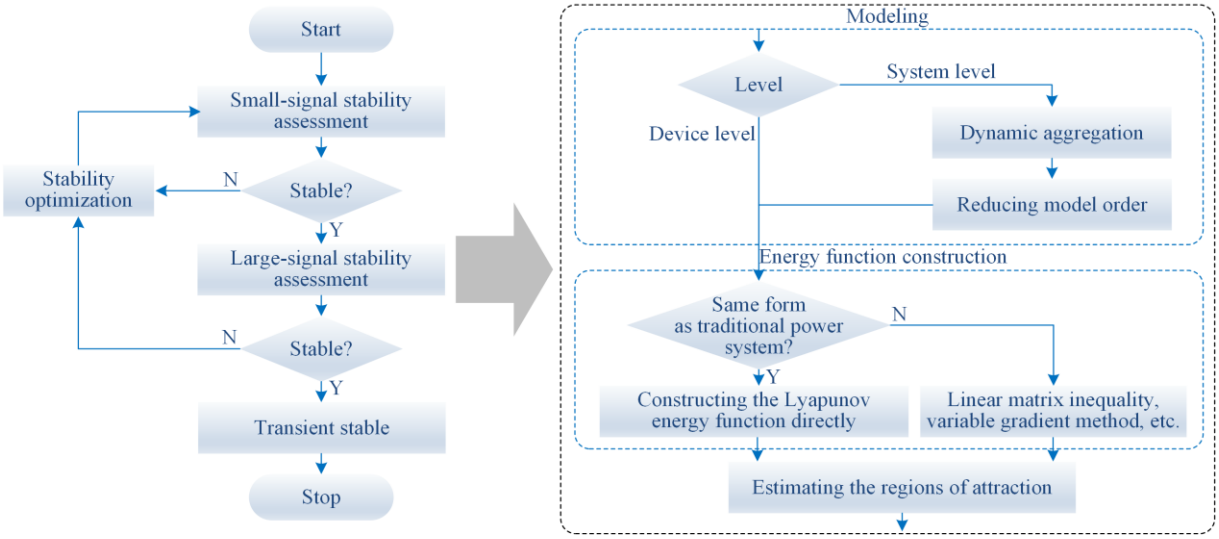

Fig. 9. An assessment framework for the large-signal stability of the microgrid [32], [35], [42].

Construction of the Lyapunov function: Building an appropriate energy function $V(x)$ is the key to analyzing transient stability [70]. However, $V(x)$ cannot be built directly because of the special form of the power-electronized power system. Instead, it can be obtained implicitly by using variable gradient and linear matrix inequality (LMI) methods [32], [35], [131]. The former is an inverse method that first ensures a negative derivative of $V(x)$ around the equilibrium point and then chooses the parameters of $V(x)$. However, the solution process of this method is relatively complex and is only applicable to low-order systems [32].

On the other hand, the LMI method is to find a positive definite matrix $\boldsymbol{M}$ to satisfy that the derivative of the quadratic $V(x)=\boldsymbol{x}^{\mathrm{T}}\boldsymbol{M}_x$ is negative definite. Considering the simple form of the alternative quadratic energy functions and the convenience of numerical solutions, this method is widely used in transient stability analysis. To simplify the derivation process, the LMI iterative algorithm is presented in [78], [132]. For each nonlinear term in the state matrix $\boldsymbol{A}$, the algorithm is to set its maximum and minimum values. Thereby, 2^r matrices $\boldsymbol{A}_i$ can be obtained when there are r nonlinear terms in the state matrix $\boldsymbol{A}$. Finally, these matrices are verified to satisfy the following LMI:

$$\begin{cases} \boldsymbol{M}=\boldsymbol{M}^{\mathrm{T}}>0 \\ \boldsymbol{A}_i^{\mathrm{T}}\cdot\boldsymbol{M}+\boldsymbol{M}\cdot\boldsymbol{A}_i<0,\ \forall i\in\{1,\ 2,\cdots,\ 2^r\} \end{cases} \tag{30}$$

When $\boldsymbol{A}_i$ satisfies (30), it indicates that the system has local asymptotic stability. As the algorithm is executed, the nonlinear term is continuously adjusted until (30) is no longer satisfied. Finally, the positive definite matrix $\boldsymbol{M}$, the energy function $V(x)=\boldsymbol{x}^{\mathrm{T}}\boldsymbol{M}_x$, and the limit values of nonlinear terms are obtained together.

Domain of attraction estimation: If a point in a specific region of the state space is taken as the initial running point, and the system can be "attracted" to the equilibrium state through a transient process, then this region can be called the DOA [35]. When the average model is used for transient stability analysis at subsystem and global system levels, the DOA of the nonlinear system is shown in Fig. 10, where x_i is an equilibrium point of the system before the fault. When $t=t_0$, the system suffers a large disturbance, and the running point deviates from x_i, while when $t=t_c$, the fault is cleared, and the system returns to the equilibrium state x_e if the state x is within the DOA of x_e. Otherwise, the system will disperse and destabilize. On the other hand, the critical time t_c can also be obtained after determining or estimating the DOA.

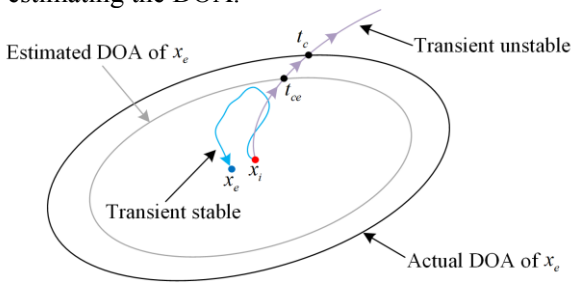

Fig. 10. Estimation of the domain of attraction for nonlinear systems [35].

However, the exact DOA is difficult to obtain with an analytical approach. Therefore, in practice, the LMI method, unstable equilibrium point method, etc., are usually used to approximate the DOA [35]. The former method transforms the DOA estimation into a convex optimization problem, which is easy to solve numerically. However, this approach is based on Lyapunov analysis, and the estimations are usually conservative [78]. The latter method works by finding unstable equilibrium points with minimum Lyapunov function values and defining such point collection as the maximum level set, which is then used to estimate the system attraction domain. However, it is difficult to calculate all the unstable equilibrium points, and the existence of these points cannot be guaranteed on the boundary of the DOA [35].

The direct methods do not need to analyze and solve the nonlinear differential equations of the system. Unlike the time-domain simulation methods, it is fast in calculation and can quantitatively evaluate the stability margin of power systems through energy functions [133]. On the other hand, compared with small-signal stability analysis methods, the direct method has the following advantages [3]: 1) The effectiveness and available range of the direct method are greater than those of small-signal stability analysis methods; 2) It is more suitable to reflect the nonlinear characteristics of power electronics converters; and 3) Large disturbances in renewable energy such as photovoltaic solar and wind energy can be fully considered. In the meantime, there are some challenges in the application of the direct method: 1) It is not easy to find the proper Lyapunov function; 2) Applications in unbalanced three-phase systems need to be verified; 3) Few existing studies have considered the dynamic interactions between power electronics converters and electromechanical systems; 4) Lack of systematic mathematical modeling methods that can be widely used for different generators and loads; and 5) Modeling MG systems as non-autonomous or time-varying systems is a challenging and important issue.

c) Other Methods

In addition to the above two common analysis methods, the large-signal stability analysis methods also include hybrid, inverse trajectory and semi-tensor product methods. The hybrid method combines the time-domain simulations and Lyapunov methods. First, the time response curve of the system state is obtained through time-domain simulations, and then the energy of the system is calculated according to the curve trajectory, and finally, the power angle stability of the system is evaluated. This method has advantages in the online monitoring of power systems and has a good reference value for transient stability analysis in MG systems [32]. Based on an asymptotically stable region obtained, the inverse trajectory method obtains that trajectory by integrating the points on the boundary of the region and estimates the stable boundary with the set of these trajectories. The DOA can be predicted by this method without requiring the system dynamics to be identified, so it is easy to be applied to systems with more states [134]. However, in addition to accuracy, this method also needs to consider the computation demand and implementation difficulty when the order of the system is very high. Therefore, the practicability of this method in high-order systems needs to be improved. The semi-tensor product method directly determines the stability of nonlinear systems through the semi-tensor product of a multi-variable multinomial. The main advantage of this method is that it can evaluate the stability of the system and estimate the boundary of the region of attraction without building the transient energy function. Similar to the inverse trajectory method, this method is also constrained by the order of the system and is only limited to low-order systems currently [32].

3) Stability Analysis Based on Timescale Decomposition

Considering the multi-timescale dynamical coupling behavior of MG systems, it is difficult to identify one timescale as a benchmark to describe all dynamic behaviors of the system. This poses great difficulties for

stability analysis. In the transition analysis of the MGC system based on angular droop control provided in [45], the nonlinear transient process is divided into fast and slow subprocesses, as shown in Fig. 11. It is worth noting that transient and quasi-steady-state analysis methods can be used for the analysis of fast-approaching and asymptotically converging slow subprocesses, respectively. To further strengthen the correlation between transient and quasi-steady-state analysis, a stability analysis method with a timescale decomposition algorithm is proposed and improved in [47], [51], [53]. By integrating the stability assessment of the fast and slow subsystems through a generic algorithm, this method can effectively identify the unstable modes of the system. A detailed description of the fast and slow subsystem models in this method is:

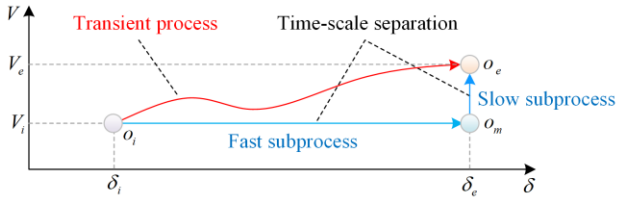

Fig. 11. Decomposition of the transient process on timescales [45].

The model of the slow subsystem: First, the system model in this method is expressed as the singularly perturbed form of (26). Assume (x_0, z_0) and (x_s, z_s) are the initial running point and asymptotic equilibrium point of the system Σ_ε, respectively, and $\varphi_\varepsilon(t, x_0, z_0)$ is the trajectory of Σ_ε. Then, $A_\varepsilon(x_s, z_s) = \{(x,z) \in R^n \times R^m : \varphi_\varepsilon(t, x_0, z_0) \to (x_s, z_s) \text{ as } t \to \infty\}$ is the stability region of (x_s, z_s). Letting $\varepsilon \to 0$ in (26), the model of the slow subsystem Σ_ε is obtained as:

$$(\sum_0)\begin{cases} \dfrac{dx}{dt} = f(x,z) \\ 0 = g(x,z) \end{cases} \tag{31}$$

Under the constraint of $g(x,z) = 0$, a new state variable space $\Gamma = \{(x,z) \in R^n \times R^m : g(x,z) = 0\}$ is obtained. Again, assume $\varphi_0(t, x_0, z_0)$ as the trajectory of the slow subsystem Σ_0, then $A_0(x_s, z_s) = \{(x,z) \in \Gamma : \varphi_0(t, x_0, z_0) \to (x_s, z_s) \text{ as } t \to \infty\}$ is the stable region of Σ_0 at (x_s, z_s).

The model of the fast subsystem: Defining the fast timescale $\tau = t/\varepsilon$, a new form of (26) is obtained as:

$$(\prod_\varepsilon)\begin{cases} \dfrac{dx}{d\tau} = \varepsilon f(x,z) \\ \dfrac{dz}{d\tau} = g(x,z) \end{cases} \tag{32}$$

Let $\varepsilon \to 0$ in (32), which means the time is scaled, x is approximated as its constant x_0, and the model of the fast subsystem $\Pi_F(x)$ is obtained as:

$$(\prod_\varepsilon)\begin{cases} \dfrac{dx}{d\tau} = \varepsilon f(x,z) \\ \dfrac{dz}{d\tau} = g(x,z) \end{cases} \tag{33}$$

In (33), (x, z) is regarded as an equilibrium point of $\Pi_F(x)$ if and only if $(x,z) \in \Gamma$. Again, assume $\Phi_0(\tilde{x}(\tau) \equiv x_0, \tilde{z}(\tau, x_0, z_0))$ as the trajectory of $\Pi_F(x)$, then, $A_F(x_0, z^*) = \{z \in R^m : \Phi_0(\tau, x_0, z_0) \to (x_0, z^*)$ as $\tau \to \infty\}$ is the stable region of $\Pi_F(x)$ at (x_0, z^*). In fact, the effectiveness of this approach is based on the following three assumptions, which are proved in [47], [51].

Assumption 1: The stability of the fast-and slow-subsystems implies the stability of the two-timescale system.

Assumption 2: Instability of the fast subsystem implies instability of the two-timescale system.

Assumption 3: Instability of the slow subsystem implies instability of the two-timescale system.

The general flow of the timescale decomposition algorithm to system stability analysis is shown in Fig. 12. The algorithm assumes that after the system is subjected to perturbations or faults, the topology of the system changes because of control or protection switching actions, resulting in a new dynamic system. In the stability analysis of such new dynamic systems, it always starts with the evaluation of the stability of the fast subsystem and continues to the slow subsystem if the fast subsystem is stable. If both the fast and slow subsystems are stable, the stability of the original system can be ensured by Assumption 1. Generally, the stability conclusion of the original system can be guaranteed when the system is not subjected to further switching actions [47]. To ensure the stability of the system, the algorithm needs to be further verified so that no bifurcations of fast equilibrium points occur due to the variation of slow dynamics in the time involved in the analysis [51].

As a global analysis tool, the timescale decomposition technique combines traditional quasi-steady-state and transient analysis. It means that this method can provide a more macroscopic view of the dynamic behavior and unstable modes of the system, and allow a more practical evaluation of the stability region. In terms of numerical computations, this method has a high degree of freedom in subsystem division and integration step selection, and thus has a good potential to improve analysis efficiency. The study on the interactions between the fast and slow dynamics of the power systems such as the natural-gas hybrid MG [52] and wind-diesel hybrid MG [51] by using this method has been presented, avoiding the erroneous conclusions obtained from the quasi-steady-state and transient analysis, respectively.

A comparison of the timescales and merits and drawbacks of the various methods for dynamic stability analysis of MGs is summarized in Table IV.

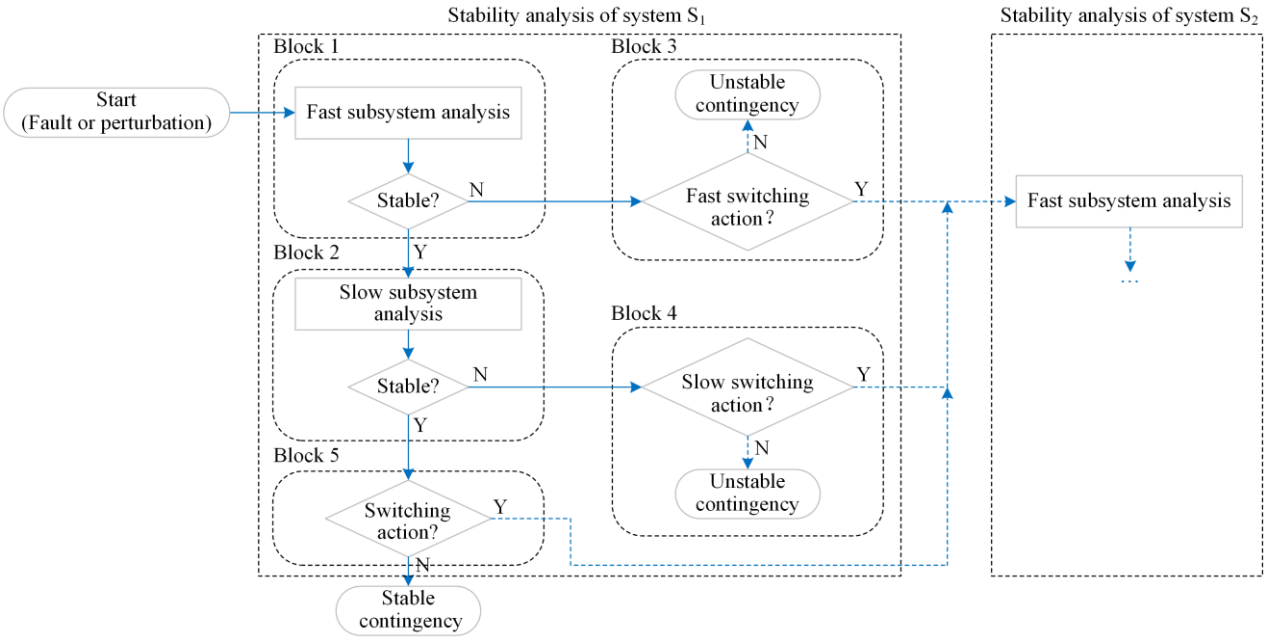

Fig. 12. Flow chart of the general algorithm for stability analysis based on timescale decomposition [47].

TABLE IV
COMPARISON OF DIFFERENT METHODS FOR DYNAMIC STABILITY ANALYSIS OF A MICROGRID

Methods		Effective timescale	Merits	Drawbacks
Small-signal stability analysis	Eigenvalue analysis [6], [77], [81]	Slow-scale	√ Simple principles and rigorous criteria √ Provide extensive information on system characteristics and stability margins	× Accuracy depends on system parameters × Higher-order models containing interactions are complex to build and analyze
	Impedance analysis [34], [42], [80], [135]		√ Low dependence on internal system parameters √ Low computational complexity √ Greater practicality and visibility	× Modeling the impedance of grid-connected inverters is difficult × Analytical conclusions may change as the nodes change × Stability of individual devices cannot be analyzed
	Time-domain simulation [31], [45], [105], [111], [116], [121], [126], [136]	Fast-scale	√ Mature technology and high practicality √ High reliability and validity of conclusions √ Often used as a test for other analytical methods	× Slow numerical integration and inefficient computation in higher-order systems × Simulation model needs to be updated as system state changes × No quantitative information on the system stability margin is available × Lack of insight into the instability mechanisms
Large-signal stability analysis	Direct method [45], [70], [120], [121], [133], [136], [137]		√ Fast computations √ Quantitatively assess system stability margins	× Accuracy depends on the construction of energy functions
	Hybrid method [32], [35]		√ Often used for transient stability analysis of conventional power systems	× Larger calculations in large-scale systems
	Inverse trajectory method [134]		√ No need to identify system dynamics	× Inverse integration cannot be performed for all points on the boundary × Only for low-order systems
	Semi-tensor product method [32], [35]		√ No need to construct a transient energy function for the system	× Only for low-order systems
Stability analysis based on timescale decomposition [45], [47], [51]–[53]		Two timescales	√ Deeper insight into dynamics and instability modes of multi-timescale systems √ Less conservative estimates of stability regions and critical clearing times √ High analytical efficiency	× Accuracy depends on the division of the fast and slow subsystems

C. Verification

In this part, large and small-signal modeling and stability analyses are performed for an islanded AC MG system with the discussed cascaded implemented configuration. The system architecture includes two inverters and two linear loads, as shown in Fig. 13, which is a typical source-network-load structure [99]. A droop control structure, including power, voltage, and current controllers, is used in each inverter, as previously shown in Fig. 4. For simplicity, all inverters have identical control parameters while feeding linear loads, and all system parameters are listed in Table V.

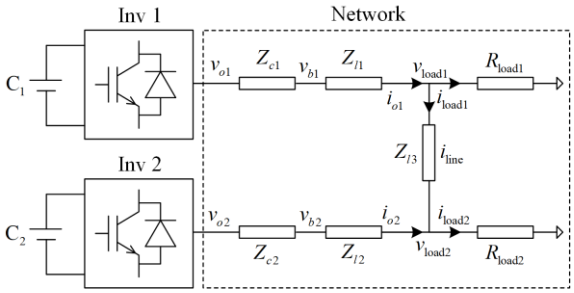

Fig. 13. System structure of AC MG with two inverters and two resistive loads [97].

TABLE V
SYSTEM MAIN PARAMETERS OF MICROGRID [76], [79], [97]

Symbol	Description	Values
S_b	Rated power (Inv1, Inv2)	10 kVA
ω_n	Nominal frequency	314 rad/s
V_n	Nominal phase-phase voltage	380 V
L_f	Filter inductance	1.35 mH
R_f	Series resistance of L_f	0.1 Ω
C_f	Filter capacitance	50 μF
ω_c	Filter cut-off frequency	31.41 rad/s
m_p	Default P-ω droop gain	9.4×10^{-5} rad/s/W
n_q	Default Q-V droop gain	1.3×10^{-3} V/Var
L_c	Coupling inductance	0.35 mH
R_c	Series resistance of L_c	0.03 Ω
C_{dc}	Capacitor of DC-side	5 F
L_{dc}	Inductor of DC-side	1 H
R_{dc}	Resistor of DC-side	1 Ω
L_l	Line inductance	0.26 mH/ km
R_l	Line resistance	0.165 Ω/ km
s_l	Line length	[0, 0, 3] km
R_{load}	Resistance of linear load	[37.2, 30] Ω

1) Small Signal Modeling and Stability Analysis

a) Full-order State-space Model and Eigenvalue Analysis

To verify the existence of interactions in multi-timescale dynamics that may lead to system instability, a linear state-space model of the case system is built in MATLAB/Simulink. With a systematic approach to constructing small-signal linearized mathematical models of droop-controlled DC/AC inverters and inverter-based MGs provided in [81], the system's mathematical, linear state-space model is built. In the modelling process, the states of power, voltage and current control, LC filter, and coupled lines and networks are considered, denoted as P_i, Q_i, δ_i, ϕ_{dqi}, γ_{dqi}, i_{ldqi}, v_{odqi} i_{odqi}, i_{linedq}, $i=1,2$. It is worth noting that the DC-side circuit of the inverter is neglected in the small-signal modeling. This will be supplemented in the next large-signal analysis.

The distribution of the system eigenvalues, as shown in Fig. 14 indicates that the system has multiple frequency components over a wide range. In [81], the results of the eigenvalue analysis indicate that the low-frequency dominant mode is highly sensitive to the power controller control parameters (m_p, n_q) related to P_i, Q_i, δ_i. Indeed, this is due to the fact that the dynamics of the power controller have mainly participated in the low-frequency dominant mode.

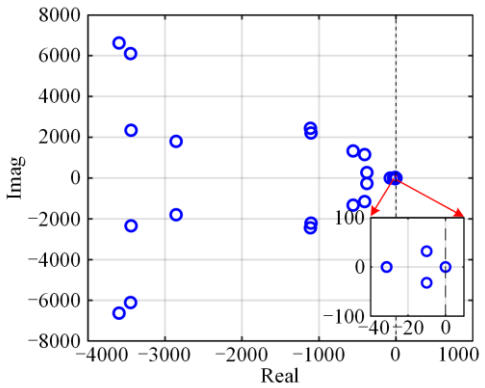

Fig. 14. Eigenvalue distribution of the described system in Fig. 13.

To verify the participation of dynamics on other timescales for low-frequency dominant modes, it further investigates the effect of relatively faster modules such as networks ($\tau = L_l/R_l = 1.58$ ms). For instance, the effect of the length of the connection line between the inverter and the PCC on the low-frequency dominant mode is illustrated in Fig. 15. To simplify the analysis, the connection line lengths (s_{l1}, s_{l2}) of inverters 1 and 2 are assumed to be the same, and the initial value of 0 represents the effective line impedance only consisting of the internal coupling impedance. In Fig. 15, it can be noted that the low-frequency dominant mode is influenced by $s_{l1,2}$, i.e., as $s_{l1,2}$ increases, the pair of conjugate poles in the low-frequency dominant mode moves away from the imaginary axis, while the damping increases, which means that the system tends to become more stable. It should be noted that a large droop gain is required to improve the transient response of DGs. This causes the low-frequency dominant mode to move towards the unstable region, thus making the system more oscillatory and eventually leading to instability. To solve this problem, a larger connection line

impedance (longer connection line) or virtual impedance control is adopted to improve the system stability region [99].

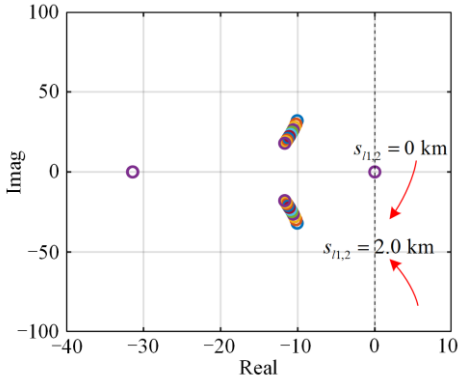

Fig. 15. Effect of the length of connection lines (0→2.0 km) on low-frequency dominant mode.

b) Model Reduction and Accuracy Verification

In fact, the above conclusions are based on the full-order model, which has many limitations in practical implementation. Therefore, a more practical scenario is considered next, where the simplified system model is used to focus only on the dominant mode. In this case, the commonly used singular perturbation reduction is used to simplify the system model. The traditional approach and the participation factor analysis are used to distinguish the fast and slow subsystems, and the ROM obtained is compared with the completed-order model (COM) in computational efficiency and accuracy.

The classification criteria for the fast dynamics of each ROM are listed in Table VI , along with the identification results and the comparison of the final computational efficiency. As for the difference in identification principles, the models obtained by the two reduction methods show differences in the identification of fast variables and, consequently, in the system order. The calculation time in Table VI is the execution time obtained by simulation calculation with the MATLAB solver. In addition, with the same system parameters and solvers, the computational time of both ROMs for 1s time-domain simulation tests is smaller than that of COM, although ROM1 is slightly smaller than ROM2. Of course, for the ROMs, the more critical issue is to ensure the dominant dynamic properties of the system to facilitate instability traceability.

TABLE VI
COMPARISON OF FAST VARIABLE IDENTIFICATION AND COMPUTATIONAL EFFICIENCY OF ROMS

Model	Principles of fast dynamic identification	Results of fast dynamic identification	Order	Solver	Calculation time (s)
COM			28	ode23	5.893
ROM1	The participation factor of low frequency dominant mode is less than 0.5%	$\phi_{dqi}, \gamma_{dqi}, i_{ldqi}, v_{odqi}\ (i=1,2)$	12	ode23	3.189
ROM2	Characteristic timescale is relatively faster	$\phi_{dqi}, i_{\text{line}dq}, \gamma_{dqi}, v_{odqi}\ (i=1,2)$	14	ode23	3.402

A comparison of the low-frequency dominant mode distribution between different models when m_p changes is presented in Fig. 16. As can be seen, compared with ROM2, the variation of the mode distribution of ROM1 is closer to that of COM, which is more effective in retaining information on the dominant timescale. When $m_p = 1.4\%$, ROM1 is as close to critical stability as COM, while ROM2 is still stable, which implies that ROM1 is more accurate in predicting the stability boundary.

The dynamic response of each model in the time domain simulation for $m_p = 0.3\%$ and 1.5% is compared in Figs. 17 and 18, respectively. For simplicity, only the rotational angular velocity ω_{com} of the reference frame, active and reactive output power P_1, Q_1 of Inverter 1 are included. In Fig. 17, all models match well when $m_p = 0.3\%$, i.e., away from the stability boundary. In Fig. 18, the difference between the models becomes significant at $m_p = 1.5\%$, i.e., crossing the stability boundary: COM and ROM1 give the correct prediction for system instability, while ROM2 gives the wrong prediction for system convergence and stability. This conclusion is also consistent with Fig. 16.

In summary, both ROMs can significantly reduce the complexity of the system model and improve computational efficiency. For the accuracy of the model, ROM2 identifies fast and slow dynamics based on the magnitude of the feature timescale and thus may fail when there are interactions between multiple timescale dynamics. On the other hand, ROM1 retains the dynamics based on the participation of the dominant mode, which is better for the dominant mode information retention and is more suitable for the analysis of multi-dynamic coupled systems.

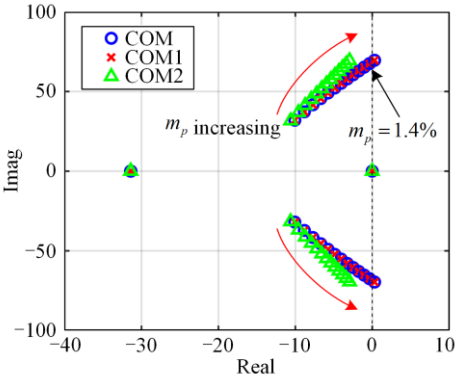

Fig. 16. Comparison of low frequency dominant modes (m_p = 0.3%−1.5%) using different modelling and method.

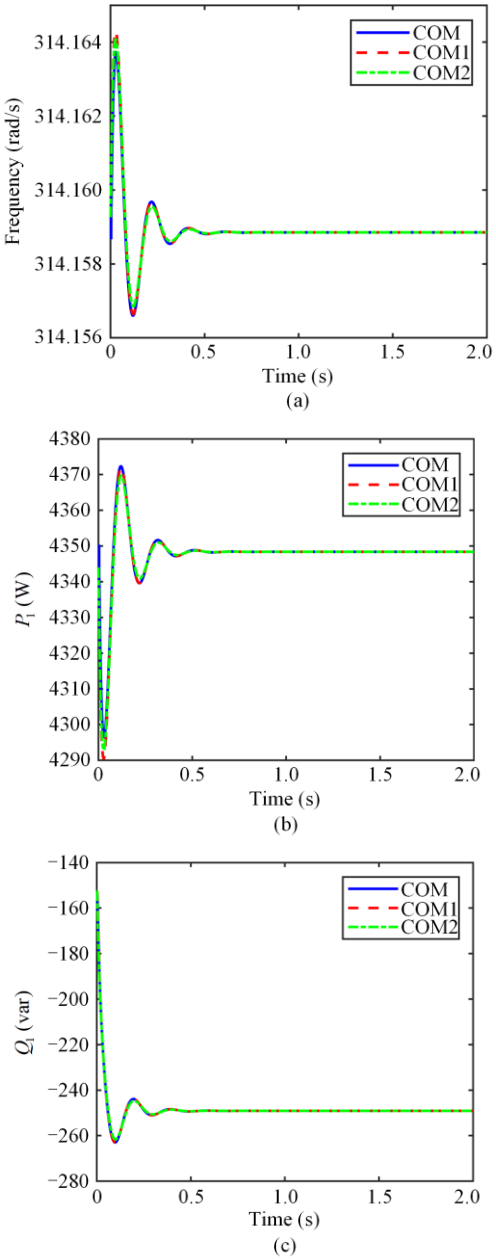

Fig. 17. Dynamic response of different models at $m_p = 0.3\%$. (a) Angular velocity ω_{com} of the reference frame. (b) Output active power P_1 of inverter 1. (c) Output reactive power Q_1 of Inverter 1 (Inv1).

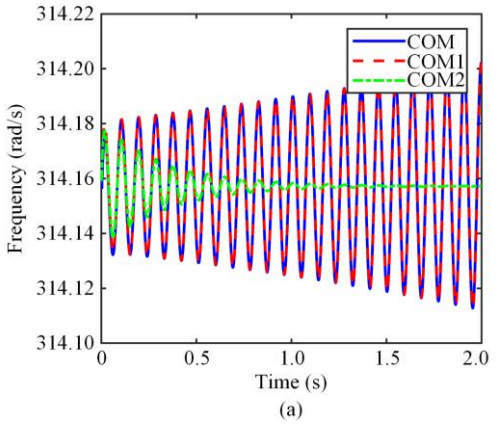

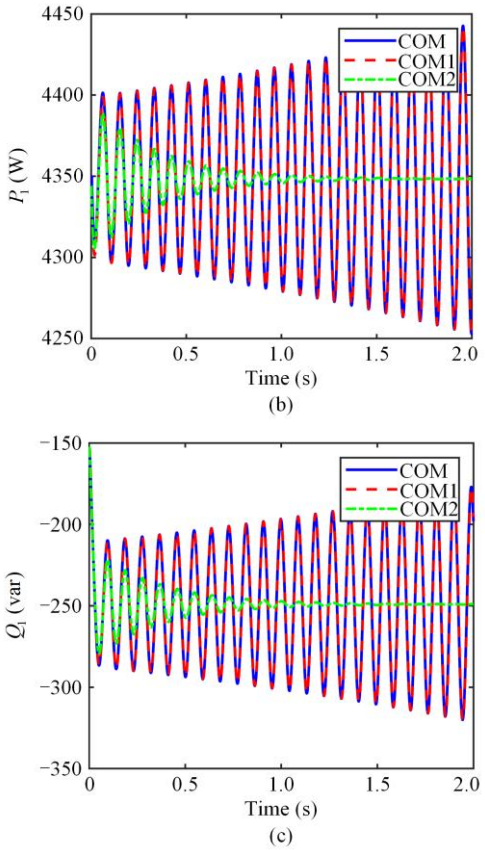

Fig. 18. Dynamic response of different models at $m_p = 1.5\%$. (a) Angular velocity ω_{com} of the reference frame. (b) Output active power P_1 of inverter 1. (c) Output reactive power Q_1 of Inverter 1 (Inv1).

2) Large Signal Modeling and Stability Analysis

The general small-signal analysis presented above is based on a linearized model, which is usually used for small perturbation cases to ensure validity. A more comprehensive and accurate assessment of AC MGs' dynamic stability can be achieved by complementing it with large-signal analysis. Thus, a nonlinear mathematical model of the case system, including the DC-side and drive circuits, is constructed in this part as a basis for large-signal stability analysis, and the DOA for the equilibrium point is estimated.

a) Establishment of Nonlinear Models and Nonlinear Terms

In the previous small-signal modeling, the DC sides of the inverters are assumed to be supplied by constant voltage sources, which neglects the correlated dynamics. However, since large DC transients exist, such as a drop in DC wind turbine output capacity due to slowing wind speed, it is necessary to analyze the effect of the DC-side circuit on the system stability. The dynamics of DC-side and drive circuits are studied in previous large-signal stability analyses [78]. Therefore, the DC-side circuit, driver, and switching circuit of the inverter, as in 0, are involved in the nonlinear model of

this part. Firstly, the nonlinear state-space model of the DC-side circuit is denoted as:

$$\begin{bmatrix} \dot{i}_{\mathrm{dc}i} \\ \dot{v}_{\mathrm{dc}i} \end{bmatrix} = \underbrace{\begin{bmatrix} -\dfrac{R_{\mathrm{dc}i}}{L_{\mathrm{dc}i}} & -\dfrac{1}{L_{\mathrm{dc}i}} \\ \dfrac{1}{C_{\mathrm{dc}i}} & 0 \end{bmatrix}}_{A_{\mathrm{dc}i}} \begin{bmatrix} i_{\mathrm{dc}i} \\ v_{\mathrm{dc}i} \end{bmatrix} + \underbrace{\begin{bmatrix} 0 \\ -\dfrac{1}{C_{\mathrm{dc}i} v_{\mathrm{dc}i}} \end{bmatrix}}_{B_{\mathrm{dc}i}(v_{\mathrm{dc}i})} [P_i] + \underbrace{\begin{bmatrix} \dfrac{V_{\mathrm{dc}i}}{L_{\mathrm{dc}i}} \\ 0 \end{bmatrix}}_{B_{2\mathrm{dc}i}} \tag{34}$$

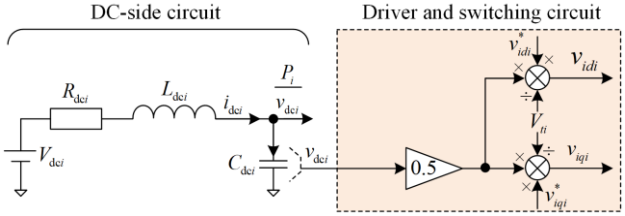

Fig. 19. DC-side and driver circuits of the inverter [76].

where $L_{\mathrm{dc}i}$, $R_{\mathrm{dc}i}$, $C_{\mathrm{dc}i}$, $V_{\mathrm{dc}i}$ are the inductance, resistance, capacitance, and the source voltage of the DC circuit of inverter i, respectively; $i_{\mathrm{dc}i}$, $v_{\mathrm{dc}i}$ are the DC current and DC voltage of inverter i, respectively. It should be noted that a certain factor of the matrix $B_{\mathrm{dc}i}$ is a function of the state variable $v_{\mathrm{dc}i}$ and is considered a nonlinear term, which differs from the linearized model. Then, in the three-phase balanced system, the driver and switching module circuits of the inverter are assumed to operate in the linear region, and the corresponding state-space model is defined as:

$$\begin{bmatrix} v_{idi} \\ v_{iqi} \end{bmatrix} = \underbrace{\begin{bmatrix} \dfrac{v_{\mathrm{dc}i}}{2V_{ti}} & 0 \\ 0 & \dfrac{v_{\mathrm{dc}i}}{2V_{ti}} \end{bmatrix}}_{\beta_i(v_{\mathrm{dc}i})} \begin{bmatrix} v_{idi}^{*} \\ v_{iqi}^{*} \end{bmatrix} \tag{35}$$

where V_{ti} is the amplitude of the triangular carrier signal of the drive circuit of inverter i; while v_{idi}^{*}, v_{iqi}^{*} are the reference signals for the voltage in the dq-frame provided by the current controller. Similarly, certain elements of the matrix $\boldsymbol{\beta}_i$ are functions that refer to $v_{\mathrm{dc}i}$. Similar to (34) and (35), the other modules of the system are modeled and finally integrated to obtain the nonlinear system model as:

$$\dot{\boldsymbol{x}}_{\mathrm{mg}} = \boldsymbol{A}_{\mathrm{mg}}(\boldsymbol{x}_{\mathrm{mg}})\boldsymbol{x}_{\mathrm{mg}} + \boldsymbol{B}_{\mathrm{mg}} \tag{36}$$

where $\boldsymbol{x}_{\mathrm{mg}}$ is the column vector composed of the system state variables; $\boldsymbol{A}_{\mathrm{mg}}$ is the system nonlinear matrix as a function about $\boldsymbol{x}_{\mathrm{mg}}$; and $\boldsymbol{B}_{\mathrm{mg}}$ is the input constant column vector. By moving the equilibrium point to the origin $\tilde{\boldsymbol{x}}_{\mathrm{mg}} = \boldsymbol{x}_{\mathrm{mg}} - \boldsymbol{x}_{\mathrm{mg}}^{e}$, where $\boldsymbol{x}_{\mathrm{mg}}^{e}$ is the equilibrium point, the system can be transformed into an autonomous system $\tilde{\boldsymbol{x}}'_{\mathrm{mg}} = \boldsymbol{A}(\tilde{x}_{\mathrm{mg}})\tilde{\boldsymbol{x}}_{\mathrm{mg}}$ [138]. For simplicity, simple linearized models can be established by assuming that the voltage and current loops of the inverter are controlled ideally with minimum perturbations. Moreover, as in [78], [81], δ_1 is set to 0 and kept constant since Inverter 1 is set as the reference frame, while δ_2 is considered small because of the small network of the case system. As a result, the non-repetitive nonlinear term in $\boldsymbol{A}(\tilde{x}_{\mathrm{mg}})$ is obtained as:

$$\begin{cases} f_1 = 1/[C_{\mathrm{dc}1} v_{\mathrm{dc}1}^{e}(v_{\mathrm{dc}1}^{e} + \tilde{v}_{\mathrm{dc}1})] \\ f_2 = \tilde{v}_{\mathrm{dc}1} \\ f_3 = \tilde{v}_{od1} \\ f_4 = 1/[C_{\mathrm{dc}2} v_{\mathrm{dc}2}^{e}(v_{\mathrm{dc}2}^{e} + \tilde{v}_{\mathrm{dc}2})] \\ f_5 = \tilde{v}_{\mathrm{dc}2} \\ f_6 = \tilde{v}_{od2} \end{cases} \tag{37}$$

b) Large Signal Stability Analysis and DOA Estimation

Based on the Takagi-Sugeno (TS) multi modeling theory and the estimation algorithm of DOA mentioned in [78], [132], the LMI solver computes $\tilde{v}_{\mathrm{dc1min}} = -497.82$ V, $\tilde{v}_{od1\min} = -190.53$ V, $\tilde{v}_{\mathrm{dc2min}} = -497.80$ V, $\tilde{v}_{od2\min} = -190.34$ V, and the corresponding positive definite matrix $\boldsymbol{M}$ is obtained. For better visualization, $V(x)$ is projected onto a 2D plane about $P_1 - Q_1$ as shown in Fig. 20(a). It can be seen that $V(x)$ is greater than 0 and has negative partial derivatives. The estimation of DOA is shown in Fig. 20(b), and the system is asymptotically stable under large-signal disturbances within the stability domain about the equilibrium point.

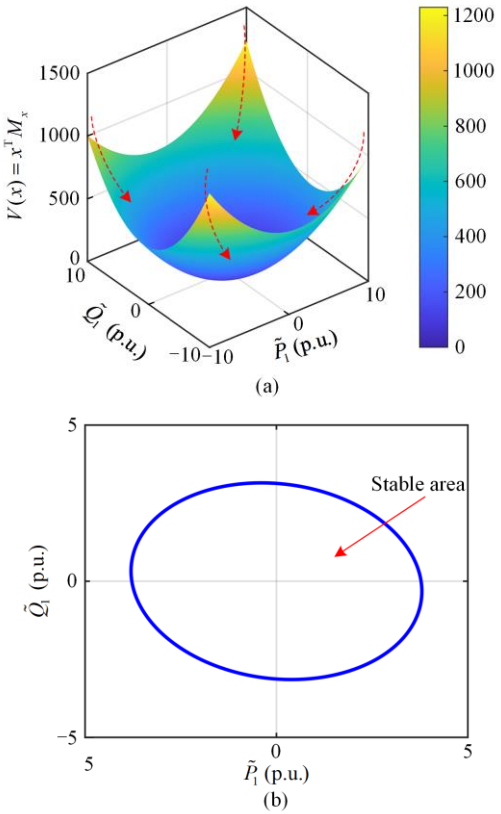

Fig. 20. Illustration of the Lyapunov function $V(x)$ and the DOA on the $P_1 - Q_1$ plane. (a) Constructed Lyapunov function. (b) DOA on the $P_1 - Q_1$ plane.

DOA variation in the P_1-Q_1 and P_2-Q_2 planes as the DC-side capacitance changes is shown in Fig. 21. In Fig. 21(a), the parameters of DC-side capacitance of Inverters 1 and 2 are set to be the same, and decrease from 5 F to 0.5 F, whereas the DOA in the P_1-Q_1 plane is significantly reduced. A similar variation of DOA is observed in the P_2-Q_2 plane in Fig. 21(b). It indicates that the DC-side capacitance has a large impact on the system stability domain even though its characteristic timescale is slower than the AC-side system.

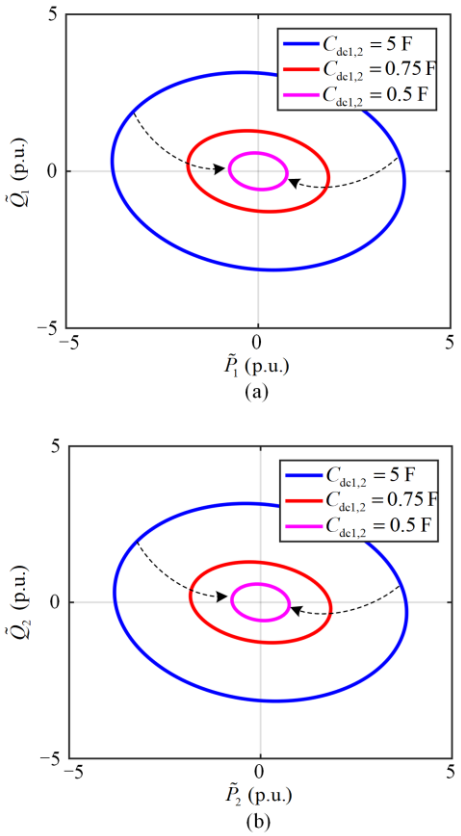

Fig. 21. Evolution of estimated DOAs with changes of the DC side capacitance C_{dc}. (a) DOAs on the P_1-Q_1 plane. (b) DOAs on the P_2-Q_2 plane.

The variations of DOA in the P_1-Q_1 plane and P_2-Q_2 plane with the change of the connection line length are illustrated in Fig. 22. To simplify the analysis, the connection line lengths of Inverters 1, and 2 are set to be the same. In Figs. 22 (a) and (b), the DOA is significantly enlarged in both the P_1-Q_1 plane and the P_2-Q_2 plane as $s_{l1,2}$ increases from 0 to 1.0 km. It means that longer connection lines have a positive effect on DOA, and the system can converge and stabilize when subjected to large signal perturbations over a larger range.

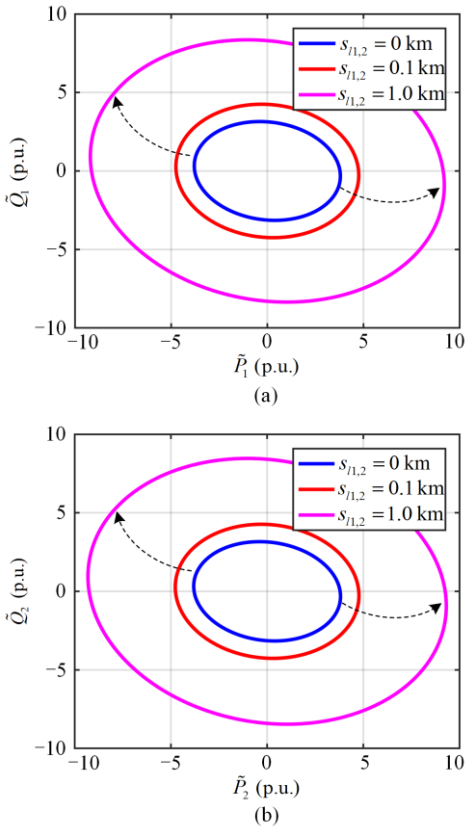

Fig. 22. Evolution of estimated DOAs with changes in the length of the connection line. (a) DOAs on the P_1-Q_1 plane. (b) DOAs on the P_2-Q_2 plane.

V. Discussion on Future Trends

Compared with traditional power systems, MGs have the advantages of flexible controllability, high energy potential utilization efficiency, small transmission loss, better environmental impact, etc., and are one of the potential major development trends of power systems in the future. With the in-depth study of AC MGs in recent decades, the problems of system control and stability, to a certain extent, have been solved. However, some challenges still need to be tackled before MG technologies can reach their full potential, and the future directions of work are summarized as follows:

A. Trends in Control Strategies for the AC MG

The future trends of MGs' control strategy are mainly related to energy services and protection, including demand response, optimal power flow, market participation, energy storage management, etc. [62]. With the expansion of the capacity and scale of the MG, the system has a large number of controllable resources, and the power flow is not limited to only one direction. This increases the requirements for the performance of voltage/frequency regulation and power flow control. Therefore, hierarchical control, which coordinates multiple timescales and multiple types of components on the basis of a multi-level data network, is used to

ensure the reliable and economic operation of the MG [19]. In the hierarchical control structure, distributed control is more equalized and decentralized than with centralized control, with greater applicability and flexibility, especially in applying voltage and frequency secondary recovery [139]–[141], while conforming to the development trend of open and flat systems. However, the coordinated operation of hierarchical control structures is highly dependent on communication links, and thus, low-cost, low-latency, and high-reliability information communication networks are important research directions for future MGs and MGCs [26].

In AC MGs including CPL, suppressing oscillations to maintain system stability is still a concern for MG control technology. To eliminate the negative effects of CPL, hardware measures such as resistive loads, filters, and energy storage systems are suggested [142]. Some typical linear stabilization control strategies, such as active and passive damping techniques, are also applied to suppress system oscillations [143]. However, the linearization nature has confined their validity to a small neighborhood of predefined system steady-state operating points. To cope with the large-signal changes in load, which are prevalent in AC MGs in practical application, nonlinear controls such as sliding mode control and model predictive control are suggested to accommodate the wide range of input voltage and power variations [144]–[147]. However, there still exist some challenges in eliminating the computational stress of nonlinear controllers and the effects of measurement noise and model uncertainty. To overcome these drawbacks, some fuzzy logic controllers, which do not require all system states to calculate the control inputs, have good computational speed and robustness [148], [149]. In [150], adaptive techniques are applied to feedback control, which further enhances the ability of fuzzy stabilizers to deal with different operating points.

Besides the management and stability control discussed above, protection systems are also necessary for AC MGs to ensure the reliable and safe delivery of electricity. Currently, the main protection schemes for MGs can be divided into two main categories [151], [152]: unit protection based on differential protection and adaptive overcurrent protection. The former has high sensitivity but requires extensive communication for real-time information exchange of fault currents and updating relay operating points dynamically, while the latter adjusts the protection parameters accordingly by tracking MG status and has fewer communication loads but is less sensitive. Moreover, a hybrid protection scheme that coordinates various existing protections in MG through a central controller is proposed in [151], which improves the accuracy and precision of the protection scheme in general and has low retrofitting costs. Notably, implementing multiple protection schemes in a single grid makes it possible to gradually upgrade from existing legacy systems.

B. Trends in Modeling Methods for the AC MG

In the stability analysis of the MG, mathematical modeling is a critical step in analyzing the new types of instability and improving the efficiency of the analysis. However, in previous MG system stability analyses, it is difficult to balance multi-timescale characteristics and coupling retention in modeling, and no unified model has been established. In addition, the following key factors have not been adequately considered in the modeling of MG systems: 1) multiple operating conditions of DGs [9]; 2) DC-side dynamics and dead-time effect of inverters [78], [153]; 3) dynamic interactions on multiple timescales [50]; and 4) equivalent models for complex loads such as nonlinear and unbalanced loads [6], [119], [154], [155]. Because of the diversity of power generation, loads, and equipment suppliers, there is a growing demand for adaptable and standardized modeling methods for MG systems [36], [46].

Standardized model simplification methods for DG/load clusters and networks remain a potential area for further investigation, as the scalability and applicability of models for the subsystem and system-level stability analysis of MGs face significant challenges [36], [46]. Moreover, in the process of model simplification, errors caused by ignoring certain dynamics and parameters are unavoidable, and thus the model simplification methods with high-precision and modeling error prediction methods are also important research directions [99].

C. Trends in Stability Analysis of the AC MG

As the main approach of integrating new energy sources into the grid, the uncertainty, complexity, and vulnerability of MG systems will become more prominent in future development. New forms of interaction stability problems, such as broadband oscillations, as well as traditional voltage and frequency regulation and stability issues, will also become more critical, increasing the need for a better understanding of the instability mechanisms of MG systems. Currently, the small-signal stability of AC MGs with various conventional control structures and operating conditions has been studied extensively. However, with the wide application of hierarchical controls in MG systems, the need to analyze the stability of this control system becomes more and more urgent [27], [156]. The advantages of distributed control have been widely discussed, but its impact on the performance and stability of MGs, especially in the case of communication delays, has not been properly studied [89], [91], [157]. The effect of the DC-side dynamics of the inverters on the small-signal stability of the system also needs to be

further investigated because of the intermittent and random nature of renewable energy sources.

Compared with the depth and scope of small-signal stability analysis in AC MGs, the current studies of transient problems are scenario-specific without any benchmark system [92]. It is necessary to study the influence of topologies, control parameters, and operating conditions on the stability domain to optimize the operation of the MG system [90], [158]. For multi-timescale and strong nonlinear systems such as MGs, it is essential to consider multi-timescale dynamics and their interactions in stability analysis, but whether the large-signal stability analysis can be used to analyze such issues remains to be explored [48]. To simplify the analysis of the system, the influence of the DC-side dynamics of inverters on large-signal stability is often neglected, and this needs to be elucidated in future studies [78]. Also, when analyzing the instability phenomena caused by dynamic interactions between the fast and slow dynamics of the system, the accuracy of the stability conclusions obtained by the large- and small-signal stability analysis still needs to be verified. In the exploration of the dynamic behaviors of multi-timescale systems, the stability analysis based on timescale decomposition seems to be a feasible research method, but the method is currently limited to small-scale hybrid dynamic systems and has not yet been extended to MGCs and larger complex power systems.

VI. Conclusion and Recommendations

This paper presents an overview of hierarchical control architecture, modeling approaches, and stability analysis methods in AC MGs with dynamic interactions on multiple timescales. In such power-electronized power systems as MGs, there are many state variables involving a wide range of timescales, and there may be coupling between these state variables with strong nonlinearities, thus presenting dynamic stability problems differing from those of traditional power systems. Considering the increasing size of MG systems due to the utilization of new energy sources and potential limitations in control hierarchy design, the dynamic interactions between multiple timescales become increasingly significant, threatening the reliable and economical operation of the system. Traditional perceptions and analysis of power system stability are based on a single timescale and ignore the coupled interactions between electrical components, and thus the applicability of traditional system modeling and analysis methods for MG systems needs to be verified. To explore multi-timescale characteristics and cognize instability mechanisms of MG systems, this paper provides a definition and classification of the dynamic stability of MG systems and discusses the applicability of various modeling approaches and stability analysis methods from a timescale perspective. Simulation verifications have also been implemented for performance comparison. Finally, the development trends of the control technology, modeling, and stability analysis in MGs are discussed and prospected, while the MG technology still has a broad development space. Further recommendations can be applied to this study, such as multi-timescale modeling and dynamic stability analysis for hybrid AC/DC interconnected MGs with high penetration of renewable energy sources.

Acknowledgment

Not applicable.

Authors' Contributions

Mingyue Zhang: conceptualization, methodology, data curation, software, original draft preparation. Yang Han: conceptualization, methodology, data curation, reviewing, and editing. Yuxiang Liu: conceptualization, methodology, data curation, software, original draft preparation. Amr S. Zalhaf: conceptualization, methodology, reviewing, and editing. Ensheng Zhao: methodology, reviewing and editing. Karar Mahmoud: reviewing and editing. Mohamed M. F. Darwish: reviewing and editing. Frede Blaabjerg: reviewing and editing. All authors read and approved the final manuscript.

Funding

This work is partly supported by the National Natural Science Foundation of China (NSFC) (No. 51977026), the Science and Technology Program of Sichuan Province (No. 2021YFG0255), and the Sichuan Provincial Postdoctoral Science Foundation (No. 246861).

Availability of Data and Materials

Not applicable.

Declarations

The authors declare that they have no known competing financial interests or personal relationships that could have appeared to influence the work reported in this paper.

Authors' Information

Mingyue Zhang received the M.S. degree in control engineering from Xi'an Polytechnic University in 2022. He is currently working toward the Ph.D. degree in control science and engineering with the School of Mechanical and Electrical Engineering, University of Electronic Science and Technology of China, Chengdu, China. His research interests include power system operation and control, computer technology and applications, and analysis of new power system.

Yang Han received the Ph.D. degree in electrical engineering from Shanghai Jiaotong University (SJTU), Shanghai, China, in 2010. In 2010, he joined the University of Electronic Science and Technology of China (UESTC), Chengdu, China, where he has been an associate professor, in 2013, and full professor, in 2021. From March 2014 to March 2015, he was a visiting scholar with the Department of Energy Technology, Aalborg University, Aalborg, Denmark. He has published a book *Modeling and Control of Power Electronic Converters for Microgrid Applications*, ISBN: 978-3-030-74512-7 (Springer). He was listed as "World Top 2% Scientist 2020" by Stanford University since 2020 and the recipient of the Young Scientist Award in CPESE 2021, the Provincial Science and Technology Award in 2020, Science and Technology Award from Sichuan Electric Power Company in 2019, Academic Talent Award by UESTC, in 2017, and Baekhyun Award by the Korean Institute of Power Electronics, in 2016.

Yuxiang Liu received the B.E. degree in electrical engineering from University of Electronic Science and Technology of China (UESTC), Chengdu, China, in 2019 and the M.S. degree in electrical engineering from University of Electronic Science and Technology of China (UESTC), Chengdu, China, in 2022. His research interest includes the stability analysis of AC/DC microgrids, HVDC, and analysis of new power system.

Amr S. Zalhaf was born in Tanta, Egypt, in 1988. He received the B.Sc. and M.Sc. degrees in electrical engineering from Tanta University, Tanta, Egypt, in 2010 and 2014, respectively, and the Ph.D. degree in energy resources engineering from Egypt-Japan University of Science and Technology (E-JUST), Alexandria, Egypt, in 2019. Since 2010, he has been with the Faculty of Engineering, Tanta University, where he became an Assistant Professor in 2019. He was a visiting scholar with the Department of Electrical and Electronic Engineering, School of Engineering, Tokyo Institute of Technology, Tokyo, Japan, in 2018. Currently, he is a post-doctoral researcher at the School of Mechanical and Electrical Engineering, University of Electronic Science and Technology of China (UESTC), Chengdu, China.

Ensheng Zhao received the B.E. degree in mechanical manufacture and automation from Inner Mongolia University for Nationalities (IMUN), Tongliao, China, in 2013. He is currently pursuing the Ph.D. degree in control science and engineering with the University of Electronic Science and Technology of China (UESTC), Chengdu, China. His research interest includes the control strategy and stability analysis of AC/DC microgrids, PV, DFIG, HVDC, and renewable energy systems.

Karar Mahmoud received the B.Sc. and M.Sc. degrees from Aswan University, Aswan, Egypt, in 2008 and 2012, respectively, both in electrical engineering, and the Ph.D. degree from the Electric Power and Energy System Laboratory (EPESL), Graduate School of Engineering, Hiroshima University, Hiroshima, Japan, in 2016. Since 2010, he has been with Aswan University, where he is currently an assistant professor with the Department of Electrical Engineering. He is also a postdoctoral researcher with the School of Electrical Engineering, Aalto University, Finland. His research interests include power systems, renewable energy sources, smart grids, distributed generation, optimization, application of machine learning, industry 4.0, and high voltage.

Mohamed M. F. Darwish was born in Cairo, Egypt, in 1989. He received the B.Sc., M.Sc., and Ph.D. degrees in electrical engineering from the Faculty of Engineering at Shoubra, Benha University, Cairo, in May 2011, June 2014, and January 2018, respectively. From 2016 to 2017, he joined Aalto University, Espoo, Finland, as a Ph.D. student with the Department of Electrical Engineering and Automation (EEA) and with Prof. M. Lehtonen's Group. He is currently working as an assistant professor with the Department of Electrical Engineering, Faculty of Engineering at Shoubra, Benha University. He is also a post-doctoral researcher with the Department of EEA, School of Electrical Engineering, Aalto University. His research interests include HV polymer nanocomposites, nano-fluids, partial discharge detection, dissolved gas analysis, fault diagnosis, grounding, electromagnetic fields, renewables, optimization, applied machine learning, the IoT, Industry 4.0, energy storage systems, and control systems.

Frede Blaabjerg (S'86-M'88-SM'97-F'03) was with ABB-Scandia, Randers, Denmark, from 1987 to 1988. From 1988 to 1992, he got the Ph.D. degree in electrical engineering at Aalborg University in 1995. He became an assistant professor in 1992, an Associate Professor in 1996, and a full professor of power electronics and drives in 1998 at AAU Energy. From 2017 he became a villum investigator. He is honoris causa at University Politehnica Timisoara (UPT), Romania in 2017 and Tallinn Technical University (TTU), Estonia in 2018. His current research interests include power electronics and its applications such as in wind turbines, PV systems, reliability, Power-2-X, power quality and adjustable speed drives. He has published more than 600 journal papers in the fields of power electronics and its applications. He is the coauthor of eight monographs and editor of fourteen books in power electronics and its applications e.g. the series (4 volumes) *Control of Power Electronic Converters and Systems* published by Academic Press/Elsevier. He has received 38 IEEE

Prize Paper Awards, the IEEE PELS Distinguished Service Award in 2009, the EPE-PEMC Council Award in 2010, the IEEE William E. Newell Power Electronics Award 2014, the Villum Kann Rasmussen Research Award 2014, the Global Energy Prize in 2019 and the 2020 IEEE Edison Medal. He was the editor-in-chief of the *IEEE Transactions on Power Electronics* from 2006 to 2012. He has been distinguished lecturer for the IEEE Power Electronics Society from 2005 to 2007 and for the IEEE Industry Applications Society from 2010 to 2011 as well as 2017 to 2018. In 2019–2020 he served as a president of IEEE Power Electronics Society. He has been vice-president of the Danish Academy of Technical Sciences.

REFERENCES

[1] X. Q. Fu, X. P. Wu, and C. Y. Zhang *et al*., "Planning of distributed renewable energy systems under uncertainty based on statistical machine learning," *Protection and Control of Modern Power Systems*, vol. 7, no. 4, pp. 619-645, Jan. 2022.

[2] Q. Y. He, Z. J. Lin, and H. Y. Chen *et al*., "Bi-level optimization based two-stage market clearing model considering guaranteed accommodation of renewable energy generation," *Protection and Control of Modern Power Systems*, vol. 7, no. 3, pp. 433-445, Dec. 2022.

[3] M. Farrokhabadi, D. Lagos, and R. W. Wies *et al*., "Microgrid stability definitions, analysis, and examples," *IEEE Transactions on Power Systems*, vol. 35, no. 1, pp. 13-29, Jan. 2020.

[4] A. Mohammed, S. S. Refaat, and S. Bayhan *et al*., "AC microgrid control and management strategies: Evaluation and review," *IEEE Power Electronics Magazine*, vol. 6, no. 2, pp. 18-31, Jun. 2019.

[5] L. Meng, A. Luna, and E. R. Diaz *et al*., "Flexible system integration and advanced hierarchical control architectures in the microgrid research laboratory of Aalborg University," *IEEE Transactions on Industry Applications*, vol. 52, no. 2, pp. 1736-1749, Mar.-Apr. 2016.

[6] J. W. Chen and J. Chen, "Stability analysis and parameters optimization of islanded microgrid with both ideal and dynamic constant power loads," *IEEE Transactions on Industrial Electronics*, vol. 65, no. 4, pp. 3263-3274, Apr. 2018.

[7] D. E. Olivares, A. Mehrizi-Sani, and A. H. Etemadi *et al*., "Trends in microgrid control," *IEEE Transactions on Smart Grid*, vol. 5, no. 4, pp. 1905-1919, Jul. 2014.

[8] J. A. P. Lopes, C. L. Moreira, and A. G. Madureira, "Defining control strategies for microgrids islanded operation," *IEEE Transactions on Power Systems*, vol. 21, no. 2, pp. 916-924, May 2006.

[9] Y. Peng, Z. Shuai, and X. Liu *et al*., "Modeling and stability analysis of inverter-based microgrid under harmonic conditions," *IEEE Transactions on Smart Grid*, vol. 11, no. 2, pp. 1330-1342, Mar. 2020.

[10] T. V Hoang and H. Lee, "Virtual impedance control scheme to compensate for voltage harmonics with accurate harmonic power sharing in islanded microgrids," *IEEE Journal of Emerging and Selected Topics in Power Electronics*, vol. 9, no. 2, pp. 1682-1695, Apr. 2021.

[11] A. S. Vijay, D. K. Dheer, and A. Tiwari *et al*., "Performance evaluation of homogeneous and heterogeneous droop-based systems in microgrid-stability and transient response perspective," *IEEE Transactions on Energy Conversion*, vol. 34, no. 1, pp. 36-46, Mar. 2019.

[12] D. K. Dheer, O. V Kulkarni, and S. Doolla, "Improvement of stability margin of droop-based islanded microgrids by cascading of lead compensators," *IEEE Transactions on Industry Applications*, vol. 55, no. 3, pp. 3241-3251, May.-Jun. 2019.

[13] R. C. Chen, Y. X. Yang, and T. Jin, "A hierarchical coordinated control strategy based on multi-port energy router of urban rail transit," *Protection and Control of Modern Power Systems*, vol. 7, no. 2, pp. 201-212, Apr. 2022.

[14] S. M. Alavi, and R. Ghazi, "A novel control strategy based on a look-up table for optimal operation of MTDC systems in post-contingency conditions," *Protection and Control of Modern Power Systems*, vol. 7, no. 1, pp. 4, Dec. 2022.

[15] T. K. Roy, S. K. Ghosh, and S. Saha, "Robust backstepping global integral terminal sliding mode controller to enhance dynamic stability of hybrid AC/DC microgrids," *Protection and Control of Modern Power Systems*, vol. 8, no. 1, pp. 8, Dec. 2023.

[16] M. F. Firuzi, A. Roosta, and M. Gitizadeh, "Stability analysis and decentralized control of inverter-based ac microgrid," *Protection and Control of Modern Power Systems*, vol. 4, no. 1, pp. 6, Mar. 2019.

[17] J. Lai, X. Lu, and F. Wang *et al*., "Broadcast gossip algorithms for distributed peer-to-peer control in AC microgrids," *IEEE IEEE Transactions on Industrial Electronics*, vol. 55, no. 3, pp. 2241-2251, May-Jun. 2019.

[18] Y. Wu, Y. P. Wu, and J. M. Guerrero *et al*., "AC microgrid small-signal modeling: Hierarchical control structure challenges and solutions," *IEEE Electrification Magazine*, vol. 7, no. 4, pp. 81-88, Jan. 2019.

[19] Q. Zhou, M. Shahidehpour, and Z. Li *et al*., "Two-layer control scheme for maintaining the frequency and the optimal economic operation of hybrid AC/DC microgrids," *IEEE Transactions on Power Systems*, vol. 34, no. 1, pp. 64-75, Jan. 2019.

[20] M. M. Morato, J. D. Vergara-Dietrich, and P. R. C. Mendes *et al*., "A two-layer EMS for cooperative sugarcane-based microgrids," *International Journal of Electrical Power and Energy Systems*, vol. 118, pp. 105752, Jun. 2020.

[21] A. K. Sahoo, K. Mahmud, and M. Crittenden *et al*., "Communication-less primary and secondary control in inverter-interfaced AC microgrid: an overview," *IEEE Journal of. Emerging Selected Topics in Power Electronics*, vol. 9, no. 5, pp. 5164-5182, Oct. 2021.

[22] J. M. Guerrero, M. Chandorkar, and T. Lee *et al*. "Advanced control architectures for intelligent microgrids—part I: decentralized and hierarchical control," *IEEE Transactions on Industrial Electronics*, vol. 60, no. 4, pp. 1254-1262, Apr. 2013.

[23] Z. Li, C. Zang, and P. Zeng *et al*., "Fully distributed hierarchical control of parallel grid-supporting inverters in islanded AC microgrids," *IEEE Transactions on Industrial. Informatics*, vol. 14, no. 2, pp. 679-690, Feb. 2018.

[24] P. E. S. N. Raju and T. Jain, "A two-level hierarchical controller to enhance stability and dynamic performance of islanded inverter-based microgrids with static and dynamic loads," *IEEE Transactions on Industrial. Informatics*, vol. 15, no. 5, pp. 2786-2797, May 2019.

[25] Y. Han, H. Li, and P. Shen *et al*., "Review of active and reactive power sharing strategies in hierarchical controlled microgrids," *IEEE Transactions on Power Electronics*, vol. 32, no. 3, pp. 2427-2451, Mar. 2017.

[26] Y. Han, K. Zhang, and H. Li *et al*., "MAS-based distributed coordinated control and optimization in microgrid and microgrid clusters: a comprehensive overview," *IEEE Transactions on Power Electronics*, vol. 33, no. 8, pp. 6488-6508, Aug. 2018.

[27] X. Wu, Y. Xu, and J. He *et al*., "Pinning-based hierarchical and distributed cooperative control for AC microgrid clusters," *IEEE Transactions on Power Electronics*, vol. 35, no. 9, pp. 9865-9885, Sep. 2020.

[28] Z. Zhao, P. Yang, and J. M. Guerrero *et al*., "Multiple-time-scales hierarchical frequency stability control strategy of medium-voltage isolated microgrid," *IEEE Transactions on Power Electronics*, vol. 31, no. 8, pp. 5974-5991, Aug. 2016.

[29] Y. Khayat, Q. Shafiee, and R. Heydari *et al*., "On the secondary control architectures of AC microgrids: an overview," *IEEE Transactions on Power Electronics*, vol. 35, no. 6, pp. 6482-6500, Jun. 2020.

[30] Y. A. I. Mohamed and E. F. El-Saadany, "Adaptive decentralized droop controller to preserve power sharing stability of paralleled inverters in distributed generation microgrids," *IEEE Transactions on Power Electronics*, vol. 23, no. 6, pp. 2806-2816, Nov. 2008.

[31] X. T. Yi, F. Zhao, and H. J. Cheng *et al*., "Study on transient stability of islanded microgrid with induction motor load," *Journal of Electrical Engineering*, vol. 15, no. 1, pp. 16-22, Mar. 2020.

[32] G. San, W. Zhang, and X. Guo *et al*., "Large-disturbance stability for power-converter-dominated microgrid: a review," *Renewable and Sustainable Energy Reviews*, vol. 127, p. 109859, Jul. 2020.

[33] X. M. Yuan, S. J. Cheng, and J. B. Hu, "Multi-time scale voltage and power angle dynamics in power electronics dominated large power systems," *Proceedings of the CSEE*, vol. 36, no. 19, pp. 5145-5154, Sep. 2016. (in Chinese)

[34] X. Chen, B. C. Wang, and C. Y. Gong *et al*., "Overview of stability research for grid-connected inverters based on impedance analysis method," *Proceedings of the CSEE*, vol. 38, no. 7, pp. 2082-2094, Apr. 2018. (in Chinese)

[35] S. Zhu, K. P. Liu, and L. Qin *et al*., "Analysis of transient stability of power electronics dominated power system: an overview," *Proceedings of the CSEE*, vol. 37, no. 14, pp. 3948-3962, 4273, Jul. 2017. (in Chinese)

[36] X. Wang and F. Blaabjerg, "Harmonic stability in power electronic-based power systems: concept, modeling, and analysis," *IEEE Transactions on Smart Grid*, vol. 10, no. 3, pp. 2858-2870, May 2019.

[37] L. Wang, X. C. Deng, and J. X. Hou *et al*., "A piecewise generalized state space model of power converters for electromagnetic transient efficient simulation," *Proceedings of the CSEE*, vol. 39, no. 11, pp. 3130-3140, Jun. 2019. (in Chinese)

[38] X. Yue, X. Wang, and F. Blaabjerg, "Review of small-signal modeling methods including frequency-coupling dynamics of power converters," *IEEE Transactions on Power Electronics*, vol. 34, no. 4, pp. 3313-3328, Apr. 2019.

[39] B. N. Liu, S. J. Yao, and H. Y. Zhang *et al*., "A research on multi-frequency band dynamic phasor for electromagnetic transients simulation," *Proceedings of the CSEE*, vol. 39, no. 19, pp. 5772-5781, 5905, Oct. 2019. (in Chinese)

[40] J. N. Wang, L. Wang, and X. Q. Han *et al*., "Analysis on AC/DC harmonic coupling characteristics of converter based on harmonic state space modeling," *Automation of Electric Power Systems*, vol. 44, no. 4, pp. 159-168, Nov. 2020. (in Chinese)

[41] P. Zhou, T. Q. Liu, and S. L. Wang *et al*., "Small signal modeling of LCC-HVDC station with consideration of harmonic coupling characteristics," *Power System Technology*, vol. 45, no. 1, pp.153-161, Mar. 2021. (in Chinese)

[42] R. Wang, Q. Sun, and D. Ma *et al*., "The small-signal stability analysis of the droop-controlled converter in electromagnetic timescale," *IEEE Transactions on Sustainable Energy*, vol. 10, no. 3, pp. 1459-1469, Jul. 2019.

[43] Y. Han, M. L. Yang, and H. Li *et al*., "Modeling and stability analysis of LCL-type grid-connected inverters: a comprehensive overview," *IEEE Access*, vol. 7, pp. 114975-115001, Sep. 2019.

[44] A. Suárez, C. Blanco, and P. García *et al*., "Online impedance estimation in AC grids considering parallel-connected converters," in *2018 IEEE Energy Conversion Congress and Exposition (ECCE)*, Portland, OR, USA, Sep. 2018, pp. 5912-5919.

[45] Y. Zhang and L. Xie, "A transient stability assessment framework in power electronic-interfaced distribution systems," *IEEE Transactions on Power Systems*, vol. 31, no. 6, pp. 5106-5114, 2016.

[46] M. Kabalan, P. Singh, and D. Niebur, "Large signal Lyapunov-based stability studies in microgrids: a review," *IEEE Transactions on Smart Grid*, vol. 8, no. 5, pp. 2287-2295, 2017.

[47] E. C. Pillco and L. F. C. Alberto, "On the foundations of stability analysis of power systems in time scales," *IEEE Transactions on Circuits and Systems I-Regular Papers*, vol. 62, no. 5, pp. 1230-1239, May 2015.

[48] M. Zhao, X. Yuan, and J. Hu *et al*., "Voltage dynamics of current control time-scale in a VSC-connected weak grid," *IEEE Transactions on Power Systems*, vol. 31, no. 4, pp. 2925-2937, Jul. 2016.

[49] M. H. Hemmatpour, M. Mohammadian, and A. Gharaveisi, "Simple and efficient method for steady-state voltage stability analysis of islanded microgrids with considering wind turbine generation and frequency deviation," *IET Generation Transmission and Distribution*, vol. 10, no. 7, pp. 1691-1702, May 2016.

[50] A. Navarro-Rodríguez, P. García, and J. M. Cano *et al*., "Limits, stability and disturbance rejection analysis of voltage control loop strategies for grid forming converters in DC and AC microgrids with high penetration of constant power loads," in *2017 19th European Con-*

ference on Power Electronics and Applications (EPE'17 ECCE Europe), Warsaw, Poland, Sep. 2017, pp. 1-10.
[51] E. C. Pillco, L. F. C. Alberto, and R. V. D. Oliveira, "Time scale stability analysis of a Hopf bifurcation in a wind-diesel hybrid microgrid," *IET Renewable Power Generation*, vol. 14, no. 9, pp. 1491-1501, Jul. 2020.
[52] X. Xu, H. Jia, and H. Chiang *et al*. "Dynamic modeling and interaction of hybrid natural gas and electricity supply system in microgrid," *IEEE Transactions on Power Systems*, vol. 30, no. 3, pp. 1212-1221, May 2015.
[53] Z. Zhang, Z. Chen, and Q. Bi, "Modified slow-fast analysis method for slow-fast dynamical systems with two scales in frequency domain," *Theoretical and Applied Mechanics Letters*, vol. 9, no. 6, pp. 358-362, Nov. 2019.
[54] Y. M. Ma, D. H. Zhu, and Z. Q. Zhang *et al*., "Modeling and transient stability analysis for Type-3 wind turbines using singular perturbation and Lyapunov methods," *IEEE Transactions on Industrial Electronics*, vol. 70, no. 8, pp. 8075-8086, Aug. 2023.
[55] Q. Liu, T. Caldognetto, and S. Buso, "Review and comparison of grid-tied inverter controllers in microgrids," *IEEE Transactions on Power Electronics*, vol. 35, no. 7, pp. 7624-7639, Jul. 2020.
[56] Y. Q. Zhu, L. H. Jia, and B. Q. Cai *et al*., "Overview on topologies and basic control strategies for hybrid AC/DC microgrid," *High Voltage Engineering*, vol. 42, no. 9, pp. 2756-2767, Oct. 2016.
[57] J. M. Guerrero, J. C. Vasquez, and J. Matas *et al*., "Control strategy for flexible microgrid based on parallel line-interactive UPS systems," *IEEE Transactions on Industrial Electronics*, vol. 56, no. 3, pp. 726-736, Mar. 2009.
[58] D. H. Zhu, X. D. Zuo, and S. Y. Zhou *et al*., "Feedforward current references control for DFIG-based wind turbine to improve transient control performance during grid faults," *IEEE Transactions on Energy Conversion*, vol. 33, no. 2, pp. 670-681, Jun. 2018.
[59] W. Bao, X. H. Hu, and G. H. Li *et al*., "Hierarchical control of microgrid to improve power sharing and power quality," *Proceedings of the CSEE*, vol. 33, no. 34, pp. 106-114, Dec. 2013. (in Chinese)
[60] M. J. Li, "Characteristic analysis and operational control of large-scale hybrid UHV AC/DC power grids," *Power System Technology*, vol. 40, no. 4, pp. 985-991, Apr. 2016. (in Chinese)
[61] J. Rocabert, A. Luna, F. Blaabjerg, and P. Rodríguez, "Control of power converters in AC microgrids," *IEEE Transactions on Power Electronics*, vol. 27, no. 11, pp. 4734-4749, Nov. 2012.
[62] H. Han, X. Hou, and J. Yang *et al*., "Review of power sharing control strategies for islanding operation of AC microgrids," *IEEE Transactions on Smart Grid*, vol. 7, no. 1, pp. 200-215, Jan. 2016.
[63] Q. Wan, C. J. Xia, and L. Guan *et al*., "Review on stability of isolated microgrid with highly penetrated distributed generations," *Power System Technology*, vol. 43, no. 2, pp. 598-612, Feb. 2019.
[64] R. Majumder, B. Chaudhuri, and A. Ghosh *et al*., "Improvement of stability and load sharing in an autonomous microgrid using supplementary droop control loop," *IEEE Transactions on Power Systems*, vol. 25, no. 2, pp. 796-808, May 2010.
[65] T. Qunais and M. Karimi-Ghartemani, "Systematic modeling of a class of microgrids and its application to impact analysis of cross-coupling droop terms," *IEEE Transactions on Energy Conversion*, vol. 34, no. 3, pp. 1632-1643, Sep. 2019.
[66] J. C. Vasquez, J. M. Guerrero, and M. Savaghebi *et al*., "Modeling, analysis, and design of stationary-reference-frame droop-controlled parallel three-phase voltage source inverters," *IEEE Transactions on Industrial Electronics*, vol. 60, no. 4, pp. 1271-1280, Apr. 2013.
[67] E. Lenz, D. J. Pagano, and A. Ruseler *et al*., "Two-parameter stability analysis of resistive droop control applied to parallel-connected voltage-source inverters," *IEEE Journal of Emerging and Selected Topics in Power Electronics*, vol. 8, no. 4, pp. 3318-3332, Dec. 2020.
[68] D. M. Pham and H. Lee, "Effective coordinated virtual impedance control for accurate power sharing in islanded microgrid," *IEEE Transactions on Industrial Electronics*, vol. 68, no. 3, pp. 2279-2288, Mar. 2021.
[69] D. Y. Zeng, J. Yao, and T. Zhang *et al*., "Research on frequency small-signal stability analysis of multi-parallel virtual synchronous generator-based system," *Proceedings of the CSEE*, vol. 40, no. 7, pp. 2048-2061, 2385, Mar. 2020. (in Chinese)
[70] H. H. Hong, W. Gu, and Q. Huang *et al*., "Power oscillation damping control for microgrid with multiple VSG units," *Proceedings of the CSEE*, vol. 39, no. 21, pp. 6247-6255, Apr. 2019. (in Chinese)
[71] X. Zhang, Y. Zhang, and R. Fang *et al*., "An improved virtual inductance control method considering PLL dynamic based on impedance modeling of DFIG under weak grid," *International Journal of Electrical Power and Energy Systems*, vol. 118, Jun. 2020.
[72] Y. Zhang and X. Zhang, "Statistic analysis of lightning transients on wind turbines," *Journal of Renewable and Sustainable Energy*, vol. 12, no. 6, Nov. 2020.
[73] B. S. Qin, Y. H. Xu, and C. Yuan *et al*., "The p/ω "admittance" modeling and power-frequency oscillation analysis of multi-VSGs grid-connected systems," *Proceedings of the CSEE*, vol. 40, no. 9, pp. 2923-2942, Mar. 2020. (in Chinese)
[74] K. M. Cheema, "A comprehensive review of virtual synchronous generator," *International Journal of Electrical Power and Energy Systems*, vol. 120, Sep. 2020.
[75] Q. Zhong and G. Weiss, "Synchronverters: Inverters that mimic synchronous generators," *IEEE Transactions on Industrial Electronics*, vol. 58, no. 4, pp. 1259-1267, Apr. 2011.
[76] Q. Qian, S. Xie, and L. Huang *et al*., "Harmonic suppression and stability enhancement for parallel multiple grid-connected inverters based on passive inverter output impedance," *IEEE Transactions on Industrial Electronics*, vol. 64, no. 9, pp. 7587-7598, Sep. 2017.
[77] N. Bottrell, M. Prodanovic, and T. C. Green, "Dynamic stability of a microgrid with an active load," *IEEE Transactions on Power Electronics*, vol. 28, no. 11, pp. 5107-5119, Nov. 2013.
[78] M. Kabalan, P. Singh, and D. Niebur, "A design and optimization tool for inverter-based microgrids using

large-signal nonlinear analysis," *IEEE Transactions on Smart Grid*, vol. 10, no. 4, pp. 4566-4576, Jul. 2019.

[79] V. Mariani, F. Vasca, and J. C. Vásquez *et al*., "Model order reductions for stability analysis of islanded microgrids with droop control," *IEEE Transactions on Industrial Electronics*, vol. 62, no. 7, pp. 4344-4354, Jul. 2015.

[80] S. Wang, Z. Liu, and J. Liu *et al*., "Small-signal modeling and stability prediction of parallel droop-controlled inverters based on terminal characteristics of individual inverters," *IEEE Transactions on Power Electronics*, vol. 35, no. 1, pp. 1045-1063, Jan. 2020.

[81] N. Pogaku, M. Prodanovic, and T. C. Green, "Modeling, analysis and testing of autonomous operation of an inverter-based microgrid," *IEEE Transactions on Power Electronics*, vol. 22, no. 2, pp. 613-625, Mar. 2007.

[82] I. P. Nikolakakos, H. H. Zeineldin, and M. S. El-Moursi, "Reduced-order model for inter-inverter oscillations in islanded droop-controlled microgrids," *IEEE Transactions on Smart Grid*, vol. 9, no. 5, pp. 4953-4963, Sep. 2018.

[83] Y. J. Tan, Y. Huang, and Z. Y. Yuan *et al*., "Modeling method and comparison of order reduction for micro-grid based on singular perturbation theory," *Power System Technology*, vol. 44, no. 5, pp. 1914-1923, Mar. 2020. (in Chinese)

[84] J. H. Zhang, L. Su, and R. X. Liu *et al*., "Small-signal dynamic modeling and analysis of a microgrid composed of inverter-interfaced distributed generations," *Automation of Electric Power Systems*, vol. 34, no. 22, pp. 97-102, Nov. 2010. (in Chinese)

[85] R. M. S. Filho, P. F. Seixas, and P. C. Cortizo *et al*., "Power system stabilizer for comunicationless parallel connected inverters," in *2010 IEEE International Symposium on Industrial Electronics*, Bari, Italy, Jul. 2010, pp. 1004-1009.

[86] H. J. Avelar, W. A. Parreira, and J. B. Vieira *et al*., "A state equation model of a single-phase grid-connected inverter using a droop control scheme with extra phase shift control action," *IEEE Transactions on Industrial Electronics*, vol. 59, no. 3, pp. 1527-1537, Mar. 2012.

[87] R. Han, L. Meng, and G. Ferrari-Trecate *et al*., "Containment and consensus-based distributed coordination control to achieve bounded voltage and precise reactive power sharing in islanded AC microgrids," *IEEE Transactions on Industry Applications*, vol. 53, no. 6, pp. 5187-5199, Nov. 2017.

[88] L. Chen, X. Zhu, and J. Cai *et al*., "Multi-time scale coordinated optimal dispatch of microgrid cluster based on MAS," *Electric Power Systems Research*, vol. 177, Dec. 2019.

[89] Y. Yan, D. Shi, and D. Bian *et al*., "Small-signal stability analysis and performance evaluation of microgrids under distributed control," *IEEE Transactions on Smart Grid*, vol. 10, no. 5, pp. 4848-4858, Sep. 2019.

[90] M. A. Hossain, H. R. Pota, and M. J. Hossain *et al*., "Evolution of microgrids with converter-interfaced generations: challenges and opportunities," *International Journal of Electrical Power and Energy Systems*, vol. 109, pp. 160-186, Jul. 2019.

[91] E. A. Coelho, D. Wu, and J. M. Guerrero *et al.,* "Small-signal analysis of the microgrid secondary control considering a communication time delay," *IEEE Transactions on Industrial Electronics*, vol. 63, no. 10, pp. 6257-6269, Oct. 2016.

[92] J. B. Hu, X. M. Yuan, and S. J. Cheng, "Multi-time scale transients in power-electronized power systems considering multi-time scale switching control schemes of power electronics apparatus," *Proceedings of the CSEE*, vol. 39, no. 18, pp. 5457-5467, Sep. 2019. (in Chinese)

[93] Z. J. Zeng, H. F. Xiao, and B. Gao *et al*., "Simplified small-signal modeling method of grid-connected inverters and its applications," *Proceedings of the CSEE*, vol. 40, no. 21, pp. 7002-7012, Nov. 2020. (in Chinese)

[94] V. Salis, A. Costabeber, and S. M. Cox *et al*., "Experimental validation of harmonic impedance measurement and LTP Nyquist criterion for stability analysis in power converter networks," *IEEE Transactions on Power Electronics*, vol. 34, no. 8, pp. 7972-7982, Aug. 2019.

[95] V. Salis, A. Costabeber, and S. M. Cox *et al*., "Stability assessment of power-converter-based AC systems by LTP theory: eigenvalue analysis and harmonic impedance estimation," *IEEE Journal of Emerging and Selected Topics in Power Electronics*, vol. 5, no. 4, pp. 1513-1525, Dec. 2017.

[96] H. Kim, H. Jung, and S. Sul, "Discrete-time voltage controller for voltage source converters with LC filter based on state-space models," *IEEE Transactions on Industry Applications*, vol. 55, no. 1, pp. 529-540, Jan.-Feb. 2019.

[97] X. Wu, G. Xiao, and B. Lei, "Simplified discrete-time modeling for convenient stability prediction and digital control design," *IEEE Transactions on Power Electronics*, vol. 28, no. 11, pp. 5333-5342, Nov. 2013.

[98] D. Maksimovic and R. Zane, "Small-signal discrete-time modeling of digitally controlled PWM converters," *IEEE Transactions on Power Electronics*, vol. 22, no. 6, pp. 2552-2556, Nov. 2007.

[99] P. Vorobev, P. Huang, and M. A. Hosani *et al*., "High-fidelity model order reduction for microgrids stability assessment," *IEEE Transactions on Power Systems*, vol. 33, no. 1, pp. 874-887, Jan. 2018.

[100] Y. Wang, Z. X. Lu, and Y. Min *et al*., "Small-signal analysis of micro-grid with multiple micro sources based on reduced order model in islanding operation," *Transactions of China Electrotechnical Society*, vol. 27, no. 1, pp. 1-8, Jan. 2012.

[101] E. A. A. Coelho, P. C. Cortizo, and P. F. D. Garcia, "Small-signal stability for parallel-connected inverters in stand-alone AC supply systems," *IEEE Transactions on Industry Applications*, vol. 38, no. 2, pp. 533-542, Mar.-Apr. 2002.

[102] V. Purba, B. B. Johnson, and S. Jafarpour *et al*., "Dynamic aggregation of grid-tied three-phase inverters," *IEEE Transactions on Power Systems*, vol. 35, no. 2, pp. 1520-1530, Mar. 2020.

[103] L. L. Sun, C. W. Gao, and J. Tan *et al*., "Load aggregation technology and its applications," *Automation of Electric Power Systems*, vol. 41, no. 06, pp. 159-167, Mar. 2017. (in Chinese)

[104] M. Rasheduzzaman, J. A. Mueller, and J. W. Kimball, "Reduced-order small-signal model of microgrid systems', *IEEE Transactions on Sustainable Energy*, vol. 6, no. 4, pp. 1292-1305, Oct. 2015.

[105]L. Luo and S. V Dhople, "Spatiotemporal model reduction of inverter-based islanded microgrids," *IEEE Transactions on Energy Conversion*, vol. 29, no. 4, pp. 823-832, Dec. 2014.

[106]A. Floriduz, M. Tucci, and S. Riverso *et al*., "Approximate Kron reduction methods for electrical networks with applications to plug-and-play control of AC islanded microgrids," *IEEE Transactions on Control Systems Technology*, vol. 27, no. 6, pp. 2403-2416, Nov. 2019.

[107]F. Dorfler and F. Bullo, "Kron reduction of graphs with applications to electrical networks," *IEEE Transactions on Circuits and Systems I-Regular Papers*, vol. 60, no. 1, pp. 150-163, Jan. 2013.

[108]Q. Peng, C. G. Ma, and Y. Fan, "Participation factors and contribution factors in linear modal analysis," *Power System Technology*, vol. 34, no. 2, pp. 92-96, Feb. 2010. (in Chinese)

[109]Q. R. Jiang, L. Wang, and X. R. Xie, "Study on oscillations of power-electronized power system and their mitigation schemes," *High Voltage Engineering*, vol. 43, no. 4, pp. 1057-1066, Mar. 2017. (in Chinese)

[110]B. M. Eid, N. A. Rahim, and J. Selvaraj *et al*., "Control methods and objectives for electronically coupled distributed energy resources in microgrids: a review," *IEEE Systems Journal*, vol. 10, no. 2, pp. 446-458, Jun. 2016.

[111]N. Soni, S. Doolla, and M. C. Chandorkar, "Analysis of frequency transients in isolated microgrids," *IEEE Transactions on Industry Applications*, vol. 53, no. 6, pp. 5940-5951, Nov.-Dec. 2017.

[112]M. Ahmed, L. Meegahapola, and A. Vahidnia *et al*., "Stability and control aspects of microgrid architectures-a comprehensive review," *IEEE Access*, vol. 8, pp. 144730-144766, Aug. 2020.

[113]C. J. Zhang, X. H. Wang, and H. F. Xue *et al*., "A quasi-power droop control of three-phase inverters and small signal modeling and analysis of parallel system in micro-grid," *Transactions of China Electrotechnical Society*, vol. 27, no. 1, pp. 32-39, Jan. 2012. (in Chinese)

[114]D. H. Zhu, S. Y. Zhou, and X. D. Zou *et al*., "Small-signal disturbance compensation control for LCL-type grid-connected converter in weak grid," *IEEE Transactions on Industry Applications*, vol. 56, no. 3, pp. 2852-2861, May-Jun. 2020.

[115]S. M. Ashabani and Y. A. I. Mohamed, "A flexible control strategy for grid-connected and islanded microgrids with enhanced stability using nonlinear microgrid stabilizer," *IEEE Transactions on Smart Grid*, vol. 3, no. 3, pp. 1291-1301, Sep. 2012.

[116]R. Singh and M. Kirar, "Transient stability analysis and improvement in microgrid," in *2016 International Conference on Electrical Power and Energy Systems (ICEPES)*, Aug. 2016, pp. 239-245.

[117]R. Majumder, "Some aspects of stability in microgrids," *IEEE Transactions on Power Systems*, vol. 28, no. 3, pp. 3243-3252, Aug. 2013.

[118]D. Lu, X. Wang, and F. Blaabjerg, "Impedance-based analysis of DC-link voltage dynamics in voltage-source converters," *IEEE Transactions on Power Electronics*, vol. 34, no. 4, pp. 3973-3985, Apr. 2019.

[119]E. Hossain, R. Perez, A. and Nasiri *et al*., "A comprehensive review on constant power loads compensation techniques," *IEEE Access*, vol. 6, pp. 33285-33305, Dec. 2018.

[120]D. Karimipour and F. R. Salmasi, "Stability analysis of AC microgrids with constant power loads based on Popov's absolute stability criterion," *IEEE Transactions on Circuits and Systems II-Express Briefs*, vol. 62, no. 7, pp. 696-700, Jul. 2015.

[121]H. Moussa, J. Martin, and B. Nahid-Mobarakeh, "Modeling and large signal stability analysis for islanded AC-microgrids," in *2017 IEEE Industry Applications Society Annual Meeting*, Cincinnati, OH, USA, Apr. 2017, pp. 1-6 .

[122]S. Islam and S. Anand, "Eigenvalue sensitivity analysis of microgrid with constant power loads," in *2014 IEEE International Conference on Power Electronics, Drives and Energy Systems (PEDES)*, Mumbai, India, Jan. 2014, pp. 1-6.

[123]H. Shi, F. Zhuo, and L. Hou *et al*., "Small-signal stability analysis of a microgrid operating in droop control mode," in *2013 IEEE ECCE Asia Downunder*, Melbourne, VIC, Australia, Mar. 2013, pp. 882-887.

[124]M. Ganjian-Aboukheili, M. Shahabi, and Q. Shafiee *et al*., "Seamless transition of microgrids operation from grid-connected to islanded mode," *IEEE Transactions on Smart Grid*, vol. 11, no. 3, pp. 2106-2114, May 2020.

[125]N. Asadi, M. Hamzeh, and K. Abbaskhanian, "The impact of DSTATCOM on the small-signal stability of islanded microgrids," in *2020 11th Power Electronics, Drive Systems, and Technologies Conference (PEDSTC)*, Oct. 2020, pp. 1-7.

[126]D. Mestriner, A. Labella, and M. Brignone *et al*., "A transient stability approach for the analysis of droop-controlled islanded microgrids," *Electric Power Systems Research*, vol. 187, pp. 106509, Oct. 2020.

[127]M. Kabalan, P. Singh, and D. Niebur, "Nonlinear Lyapunov stability analysis of seven models of a DC/AC droop controlled inverter connected to an infinite bus," *IEEE Transactions on Smart Grid*, vol. 10, no. 1, pp. 772-781, Jan. 2019.

[128]X. Liu and X. Sun, "Large signal stability analysis of hybrid AC/DC microgrid based on T-S fuzzy model method," in *2019 22nd International Conference on Electrical Machines and Systems (ICEMS)*, Harbin, China, Jul. 2019, pp. 1-6.

[129]V. L. Kharitonov, "Lyapunov functionals and matrices," *Annual Reviews in Control*, vol. 34, no. 1, pp. 13-20, Apr. 2010.

[130]M. Maghenem, R. Postoyan, and A. Loría *et al*., "Lyapunov-based synchronization of networked systems: from continuous-time to hybrid dynamics," *Annual Reviews in Control*, vol. 50, pp. 335-342, Jan. 2020.

[131]H. Tsukamoto, S. J. Chung, and J. J. E. Slotine, "Contraction theory for nonlinear stability analysis and learning-based control: a tutorial overview," *Annual Reviews in Control*, vol. 52, pp. 135-169, Dec. 2021.

[132]D. Marx, P. Magne, and B. Nahid-Mobarakeh *et al*., "Large signal stability analysis tools in DC power systems with constant power loads and variable power loads-a review," *IEEE Transactions on Power Electronics*, vol. 27, no. 4, pp. 1773-1787, Apr. 2012.

[133]T. X. Jia, H. D. Sun, and B. Zhao *et al*., "Research on transient stability analysis method of power system

based on network structure preserving energy function," *Proceedings of the CSEE*, vol. 40, no. 9, pp. 2819-2826, Apr. 2020. (in Chinese)

[134]B. K. Colbert and M. M. Peet, "Using trajectory measurements to estimate the region of attraction of nonlinear systems," in *2018 IEEE Conference on Decision and Control (CDC)*, Miami, FL, USA, Feb. 2018, pp. 2341-2347.

[135]B. Wen, D. Dong, and D. Boroyevich *et al*. "Impedance-based analysis of grid-synchronization stability for three-phase paralleled converters," *IEEE Transactions on Power Electronics*, vol. 31, no. 1, pp. 26-38, Jan. 2016.

[136]X. Liu, Z. Gao, and Y. Tian, "Large signal stability analysis of microgrid system based on power converter system," in *2019 22nd International Conference on Electrical Machines and Systems (ICEMS)*, Harbin, China, Jul. 2019, pp. 1-5.

[137]Y. H. Jiao, J. Bu, and N. Y. Zhang *et al*., "Transient stability analysis with VSG-IIDG power system based on energy function," *Electrotechnics Electric*, no. 3, pp. 7-11, Mar. 2019.

[138]M. H. Roos, P. H. Nguyen, and J. G. Slootweg, "Stability analysis of microgrid islanding transients based on interconnected dissipative subsystems," *IEEE Transactions on Smart Grid*, vol. 12, no. 6, pp. 4655-4667, Nov. 2021.

[139]F. Guo, C. Wen, and Y. Song, "Distributed secondary voltage and frequency restoration control of droop-controlled inverter-based microgrids," *IEEE Transactions on Industrial Electronics*, vol. 62, no. 7, pp. 4355-4364, Jul. 2015.

[140]J. W. Simpson-Porco, Q. Shafiee, and F. Dörfler *et al*., "Secondary frequency and voltage control of islanded microgrids via distributed averaging," *IEEE Transactions on Industrial Electronics*, vol. 62, no. 11, pp. 7025-7038, Nov. 2015.

[141]G. Lou, W. Gu, and Y. Xu *et al*., "Distributed MPC-based secondary voltage control scheme for autonomous droop-controlled microgrids," *IEEE Transactions on Sustainable Energy*, vol. 8, no. 2, pp. 792-804, Apr. 2017.

[142]E. Kowsari, J. Zarei, and R. Razavi-Far *et al*., "A novel stochastic predictive stabilizer for DC microgrids feeding CPLs," *IEEE Journal of Emerging and Selected Topics in Power Electronics*, vol. 9, no. 2, pp. 1222-1232, Apr. 2021.

[143]X. Li, X. Zhang, and W. Jiang *et al*., "A novel assorted nonlinear stabilizer for DC-DC multilevel boost converter with constant power load in DC microgrid," *IEEE Transactions on Power Electronics*, vol. 35, no. 10, pp. 11181-11192, Oct. 2020.

[144]H. Pan, Q. Teng, and D. Wu, "MESO-based robustness voltage sliding mode control for AC islanded microgrid," *Chinese Journal of Electrical Engineering*, vol. 6, no. 2, pp. 83-93, Jun. 2020.

[145]M. Cucuzzella, G. P. Incremona, and A. Ferrara, "Decentralized sliding mode control of islanded AC microgrids with arbitrary topology," *IEEE Transactions on Industrial Electronics*, vol. 64, no. 8, pp. 6706-6713, Aug. 2017.

[146]H. Yan, X. Zhou, and H. Zhang *et al*., "A novel sliding mode estimation for microgrid control with communication time delays," *IEEE Transactions on Smart Grid*, vol. 10, no. 2, pp. 1509-1520, Mar. 2019.

[147]T. Pippia, J. Sijs, and B. De Schutter, "A single-level rule-based model predictive control approach for energy management of grid-connected microgrids," *IEEE Transactions on Control Systems Technology*, vol. 28, no. 6, pp. 2364-2376, Nov. 2020.

[148]M. M. Esfahani, H. F. Habib, and O. A. Mohammed, "Microgrid stability improvement using a fuzzy-based PSS design for virtual synchronous generator," *IEEE SoutheastCon-Proceedings*, pp. 1-5, Jan. 2018.

[149]D. Arcos-Aviles, J. Pascual, and L. Marroyo *et al*., "Fuzzy logic-based energy management system design for residential grid-connected microgrids," *IEEE Transactions on Smart Grid*, vol. 9, no. 2, pp. 530-543, Mar. 2018.

[150]T. Hussein, M. S. Saad, and A. L. Elshafei *et al*., "Robust adaptive fuzzy logic power system stabilizer," *Expert Systems with Applications*, vol. 36, no. 10, pp. 12104-12112, Dec. 2009.

[151]T. S. Ustun and R. H. Khan, "Multiterminal hybrid protection of microgrids over wireless communications network," *IEEE Transactions on Smart Grid*, vol. 6, no. 5, pp. 2493-2500, Sep. 2015.

[152]T. S. Aghdam, H. K. Karegar, and H. H. Zeineldin, "Variable tripping time differential protection for microgrids considering DG stability," *IEEE Transactions on Smart Grid*, vol. 10, no. 3, pp. 2407-2415, May 2019.

[153]L. J. Zhang, F. Wang, and H. Guo *et al*., "Research status of resonance modeling and suppression in microgrid," *Journal of Power Supply*, vol. 14, no. 2, pp. 52-62, Mar. 2016.

[154]M. A. Allam, A. A. Hamad, and M. Kazerani *et al*., "A novel dynamic power routing scheme to maximize loadability of islanded hybrid AC/DC microgrids under unbalanced AC loading," *IEEE Transactions on Smart Grid*, vol. 9, no. 6, pp. 5798-5809, Nov. 2018.

[155]A. Arif, Z. Wang, and J. Wang *et al*., "Load modeling-a review," *IEEE Transactions on Smart Grid*, vol. 9, no. 6, pp. 5986-5999, Nov. 2018.

[156]R. Heydari, Y. Khayat, and A. Amiri *et al.*, "Robust high-rate secondary control of microgrids with mitigation of communication impairments," *IEEE Transactions on Power Electronics*, vol. 35, no. 11, pp. 12486-12496, Nov. 2020.

[157]X. Wu, Y. Xu, and J. H. He *et al.*, "Delay-dependent small-signal stability analysis and compensation method for distributed secondary control of microgrids," *IEEE Access*, vol. 7, pp. 170919-170935, Jan. 2019.

[158]A. M. Dissanayake and N. C. Ekneligoda, "Transient optimization of parallel connected inverters in islanded AC microgrids," *IEEE Transactions on Smart Grid*, vol. 10, no. 5, pp. 4951-4961, Sep. 2019.